

FOR OFFICIAL USE ONLY

JPRS L/10224

30 December 1981

USSR Report

ENGINEERING AND EQUIPMENT

(FOUO 8/81)



FOREIGN BROADCAST INFORMATION SERVICE

FOR OFFICIAL USE ONLY

NOTE

JPRS publications contain information primarily from foreign newspapers, periodicals and books, but also from news agency transmissions and broadcasts. Materials from foreign-language sources are translated; those from English-language sources are transcribed or reprinted, with the original phrasing and other characteristics retained.

Headlines, editorial reports, and material enclosed in brackets [] are supplied by JPRS. Processing indicators such as [Text] or [Excerpt] in the first line of each item, or following the last line of a brief, indicate how the original information was processed. Where no processing indicator is given, the information was summarized or extracted.

Unfamiliar names rendered phonetically or transliterated are enclosed in parentheses. Words or names preceded by a question mark and enclosed in parentheses were not clear in the original but have been supplied as appropriate in context. Other unattributed parenthetical notes within the body of an item originate with the source. Times within items are as given by source.

The contents of this publication in no way represent the policies, views or attitudes of the U.S. Government.

COPYRIGHT LAWS AND REGULATIONS GOVERNING OWNERSHIP OF MATERIALS REPRODUCED HEREIN REQUIRE THAT DISSEMINATION OF THIS PUBLICATION BE RESTRICTED FOR OFFICIAL USE ONLY.

FOR OFFICIAL USE ONLY

JPRS L/10224

30 December 1981

USSR REPORT
ENGINEERING AND EQUIPMENT
(FOUO 8/81)

CONTENTS

MARINE AND SHIPBUILDING

Design of Hydrofoil and Hover Craft..... 1

NUCLEAR ENERGY

Operating and Repairing Nuclear Power Stations..... 8

Optimization Models of Breeder Reactors..... 11

Radiation Safety in Nuclear Power Engineering..... 13

Practical Problems of Operating Nuclear Reactors..... 15

Calculating Compression of DT-Mixture by Electrically Imploded
Cylindrical Shell..... 17

NON-NUCLEAR ENERGY

Development of Turbogenerator Construction in USSR..... 26

Remote Measurement of Electrical Energy and Average Power in
Power Systems..... 37

Current State and Problems of Transformer Construction
Development..... 47

INDUSTRIAL TECHNOLOGY

Classifying Industrial Robots..... 55

- a - [III - USSR - 21F S&T FOUO]

FOR OFFICIAL USE ONLY

FOR OFFICIAL USE ONLY

NAVIGATION AND GUIDANCE SYSTEMS

Dynamics of Nonlinear Gyroscopic Systems.....	57
Programmed Angular Movements of Gyrostat When Quaternions Are Used To Determine Its Orientation.....	63
Inverse Problem of Gyroinertial Measurement Systems.....	68

- b -

FOR OFFICIAL USE ONLY

FOR OFFICIAL USE ONLY

MARINE AND SHIPBUILDING

UDC [629.124.9.039.001.2+629.124.9:533.693](031)

DESIGN OF HYDROFOIL AND HOVER CRAFT

Leningrad SPRAVOCHNIK PO PROYEKTIROVANIYU SUDOV S DINAMICHESKIMI PRINTSIPAMI
PODDERZHANIYA in Russian 1980 (signed to press 15 Jan 80) pp 2-5, 467-471

[Annotation, foreword and table of contents from book "Manual for the Design of Ships with Dynamic Principles of Support" by Boris Aleksandrovich Kolyzayev, Anatoliy Ivanovich Kosorukov and Vladilen Aleksandrovich Litvinenko, Izdatel'stvo "Sudostroyeniye", 4000 copies, 472 pages]

[Text] Fundamental information on the theory and practice of designing hydrofoil and air-cushion ships (SPK and SVP) is systematized. Methods are proposed for determining the principal dimensions of these ships, their propulsive and seakeeping qualities, and their economic characteristics. Methods of optimizing a design solution are indicated and an analysis is given of errors in calculating the basic characteristics of SPK and SVP. The principles for prescribing design margins are substantiated. Questions on the reliability and safety of these ships are elucidated.

The manual is intended for engineers and shipbuilders, specialists of NII [Scientific Research Institutes], KB [design bureaus] of shipbuilding enterprises and of the fleet. It may be used by graduate students and students of the senior courses of higher educational establishments and schools of shipbuilding.

Foreword. Ships with dynamic principles of support (SDPP); namely, SPK and SVP are winning widespread acceptance as convenient and profitable means of fast transportation.

To further perfect SPK and SVP, to improve their seakeeping qualities and increase profitability, research has been conducted over many years. In recent years works have appeared which were devoted to the hydrodynamics of hydrofoils, the aerodynamics of air cushions, the theory and practice of designing propulsors, the description of the power plants (EU) of SDPP, general and local strength, structural materials, and the analysis of experience in operating SDPP.

Among recent works, there is great interest in the books of I. T. Yegorov, N. A. Zaytsev, G. P. Zlobin, I. I. Isayev, N. V. Mattes, Yu. A. Netsvetayev, A. A. Rusetskiy, Yu. M. Sadovnikov, V. T. Sokolov, A. N. Kholodilin, A. N. Shmyrev and others.

FOR OFFICIAL USE ONLY

In the development of the theory of SVP, great contributions were made by Yu. Yu. Benua, A. N. Bagno, K. P. Vashkevich, A. D. Volkov, V. K. D'yachenko, G. P. Zlobin, V. K. Zoroastrov, T. A. Zaytsev, V. V. Klichko, B. P. Kuzovenkov, I. A. Lyubomirov, V. A. Lukashevskiy, Ye. Z. Novikov, I. V. Ozimov, V. M. Puzyrev, S. D. Prokhorov, A. A. Rusetskiy, V. N. Treshchevskiy, V. I. Khonzhonkov, V. P. Shadrin, V. V. Shatalov, V. A. Tsarev and others. Of works, however, embracing comprehensively all the knotty problems of designing SPK and SVP, there is a total insufficiency.

The book by the authors of this manual, "Features of the Design of Ships With New Principles of Support", which came out in 1974, because of an insufficient printing of copies became a bibliographic rarity and could not satisfy the inquiries of engineers and shipbuilders, teachers, graduate and undergraduate students specializing in the area of the theory of the design of ships. The text book of A. M. Vaganov, "The Design of Fast Ships", published in 1978, is a useful contribution to educational literature, but it does not cover the basic questions in the design of SPK and SVP sufficiently completely.

The manual being offered for the attention of readers makes up for the deficiency of literature on the general design of SDPP. The amount of material necessary for exploratory design studies is systematized in the book, fulfilling in the process the formation of the conception of the ship and the substantiation of the design proposal. In addition to general methods of design, recommendations are given for the formation of the function of social usefulness, for the technical and economic basis of an optimal solution, and for the design of the hydrodynamic systems, the aerodynamics of the air cushion, propulsors, and for the determination of the external forces, the stresses acting in the hull, hydrofoils, and the flexible enclosures. Recommendations on the choice of the type of power plant are given and specific numerical examples.

In many cases several formulas are presented for the determination of the same quantity. This was done on purpose. Basically, it does not work out well to give preference to any one formula when the accuracy of several of them is approximately the same. In this case, the designer, in accordance with the problems before him and an amount of initial information, can select independently from those presented the most convenient formula, or compute the sought after quantity as the average from several formulas. The formulas and charts are based on both theoretical developments and on statistically processed data from many sources. Reference data on SPKs and SVPs are presented.

The main attention was given to the choice of the general type, the principal dimensions, and the fundamental characteristics of an SDPP at the beginning of design when the fundamental properties of the ship are being defined, such as seakeeping ability, economy and others which remain essentially unchanged in the later design stages.

In the first stages of design, it is not always possible to give preference to any one type of SDPP. In a number of cases, a design is developed in several variants and only comprehensive, objective evaluation permits making a final choice for the further direction of the work. This is why it is advisable to combine in one book, data for the design of SPK and SVP.

FOR OFFICIAL USE ONLY

The book has two parts. Part I is devoted to the design of SPK, and part II to the design of SVP. Part I was written by A. I. Kosorukov. Part II, (chapters I and II) were written by B.A. Kolyzayev. Part II, (chapters V, VI, VII, and section 6 of chapter III) were written by V. A. Litvinenko. Part II, (chapter III, sections 5 and 7 of chapter IV and section 20 of chapter VI) were written by S. A. Smirnov who also assembled the material on SVP of the skeg type presented in chapter II.

The recommendations adopted by the Assembly of the International Maritime Consultative Organization (IMKO) and of the Code, which was coming into effect in 1979, on The Safety of Ships with Dynamic Systems of Support and which have an influence on the characteristics of a ship, are reflected in the manual.

The principal characteristics of SPKs and SVPs of foreign construction are presented in tables, charts, text, and drawings taken from foreign periodicals.

The book was written on the basis of the results of investigations carried out by the authors, and on the correlation of data presented in domestic and foreign literature.

The authors convey their thanks to the reviewers, candidates of technical sciences V. K. D'yachenko and B. A. Tsarev for valuable comments and recommendations directed toward improving the book. The authors also consider it necessary to express their gratitude to L. V. Ozimov, I. V. Ozimov, Ye. Z. Novikov, T. N. Belyayev, Yu. M. Mokhov, A. N. Bagno, Ye. G. Finkel'shteyn, V. K. Zoroastrov, and G. D. Baranov, whose materials and recommendations were used in writing the book.

The authors will gratefully receive comments about the contents of the manual directed to the address of the publisher, Sudostroyeniye, 191065 Leningrad, Ulitsa Gogolya 8.

Contents

	Page
Foreword.....	3
Introduction	6
Part I. The Design of Hydrofoil Ships [SPK]	
Nomenclature	11
Division I. The Bases of the General Design of SPK	15
Chapter I. Problems in the building and trends in the development of SPK....	--
1. Trends in the development of SPK	--
2. Features of SPK hull design	18
3. Features of the design of the hydrofoils	21
4. Structural materials	25
5. The fundamental characteristics of the EU [Power Plant]	28
Chapter II. Theoretical bases for the design of SPK	33
6. The methodological bases of design	--
7. Establishing the social usefulness function	35

FOR OFFICIAL USE ONLY

Chapter II (continued)	Page
8. The method of determining the fundamental characteristics of an SPK to a first approximation	39
8.1 The propulsion equation	41
8.2 The capacity equation (functional)	47
8.3 The equations of unsinkability, buoyancy, and strength	53
8.4 The weight equation (functional)	56
9. Predicting the construction and operating costs of SPK	65
9.1 The construction cost of the ship	--
9.2 The net cost of transporting passengers (cargoes)	68
10. Optimization of the characteristics of SPK	70
11. Recommendations on the scheme for calculating the characteristics of SPK to a first approximation (sample calculation)	72
12. Calculating the characteristics of SPK to a second approximation	84
12.1 Selecting the characteristics of the hydrofoil system	--
12.2 The more exact definition of hull weight	85
12.3 " " " " " the composition and weight of the power plant	86
12.4 Determining the composition of the electrical system	--
12.5 The more exact definition of fuel and lubricating oil supplies ...	--
12.6 Provisions for the safety of SPK	87
12.7 Remarks on the adjustment of SPK characteristics in the second approximation	--
Division II. The Design of the Fundamental Parts of SPK	89
Chapter III. Design of the hydrodynamic system.....	--
13. The selection of the arrangement of the hydrofoils and their geometric characteristics	--
13.1 Hydrofoil area	90
13.2 Load distribution among the hydrofoils	91
13.3 Determining the geometric characteristics of the hydrofoil system.	95
14. The hydrodynamic design of the hydrofoil system	104
14.1 Calculating hydrofoil lift	105
14.2 " " " resistance	108
15. Estimating the effect of cavitation on a supporting hydrofoil	114
16. Calculating the trim and resistance of the ship when moving on the hydrofoils	120
17. Longitudinal and transverse stability of SPK when moving on the hydrofoils	121
18. The design and calculation of propulsors	130
19. The seaworthiness of SPK	137
20. The maneuvering qualities of SPK	150
Chapter IV. Features of the hull design	152
21. Development of the lines drawing	---
22. Development of the general arrangement drawing	155
23. The problem of the external forces	159
23.1 The impact of the hull on a wave	160
23.2 " " " " " hydrofoil on the water	166
23.3 Hydrodynamic forces on a hydrofoil in regular waves	170

FOR OFFICIAL USE ONLY

Chapter IV. (continued)	page
24. Features of calculating the general strength of SPK	172
24.1 The bending moment in displacement condition	---
24.2 " " " when moving on the hydrofoils in quiet water ..	173
24.3 " " " in waves	175
24.4 The shape of the elastic line and the natural frequency of the first tone	177
24.5 The main coordinates of the bending moment and the shear force ..	180
24.6 Approximate methods of determining the bending moment in waves ..	181
25. Features of calculating the strength of the hydrofoil system	182
26. Determining the strength margins	185
Part II. The Design of Air-Cushion Ships [SVP]	
Nomenclature	191
Division I. The Bases of the General Design of SVP	195
Chapter I. Problems in the building of SVP	---
Chapter II. Theoretical bases for the general design of SVP	202
1. Methodological bases for the design of SVP	---
2. Determining the fundamental characteristics of SVP to a first approximation	203
3. Determining the principal characteristics of SVP to a second approximation	211
3.1 The weight equation	212
3.2 The stability equation	220
3.3 The power equation	---
3.4 The equation of seaworthiness	221
3.5 The equation of unsinkability	222
3.6 The capacity equation	---
4. Optimization of the characteristics of SVP	224
Chapter III. The provision for propulsive and seaworthiness qualities in the design of SVP	229
5. The transverse and longitudinal stability of SVP	---
5.1 Evaluating the stability of SVP in the different modes of operation	---
5.2 The approximate design evaluation of the static stability of SVP ..	236
6. Calculation of the resistance of SVPA [amphibious SVP]	248
7. " " " " SVPS [SVP with skegs (rigid side walls)]	276
Division II. Features of the Design of the Fundamental Parts of SVP	285
Chapter IV. Hull design	---
8. Features of SVP hull structure, Structural materials	---
9. Development of the structural strength system for an SVP hull. The calculation of general and local strength	289
Chapter V. The design of the flexible enclosures of the air cushion of SVP	298
10. The design of the flexible enclosures for SVPA	---
10.1 The classification of flexible enclosures	---
10.2 External flexible enclosures	299
10.3 Sectionalizing flexible enclosures	306
10.4 Fundamental operational requirements for the structure of flexible enclosures	307

FOR OFFICIAL USE ONLY

Chapter V (continued)	Page
11. Materials for flexible enclosures	309
11.1 The covering material for flexible enclosures	310
11.2 The textile foundation of the rubberized fabric of a material for a flexible enclosure	---
12. The design of the shape of flexible enclosures	313
12.1 The design of the shape of single-sheet monolithic elements for flexible enclosures	314
12.2 The design of the shape of two-sheet monolithic elements for flexible enclosures	317
12.3 The design of the shape of balloon type flexible enclosures	---
13. Principles for evaluating the strength of flexible enclosures	319
13.1 Features of the materials of flexible enclosures as strength members	---
13.2 Examples of calculating the strength of a single-sheet monolith ..	321
13.3 Vibrations of flexible enclosures	322
14. Determination of the flow-rate and pressure characteristics of the flexible enclosure of an air cushion	323
14.1 The lift characteristics of a nozzle-type flexible enclosure on an SVP with the ship hovering without list or trim above a hard surface	326
14.2 The lift characteristics of a flexible enclosure on an SVP hovering without list or trim above water	329
15. The influence of the design of flexible enclosures on the propulsive and seakeeping qualities of SVP	336
15.1 Amphibious SVP	---
15.2 SVP with skegs	339
Chapter VI. Fundamental questions on the design of an SVP power plant ...	341
16. Features of SVP power plants	---
16.1 General information	---
16.2 Design arrangements of the power plant	343
16.3 The main engines of SVP	345
16.4 Power transmission	346
16.5 Calculating the total engine power necessary for SVP operation ...	347
17. The design of the special systems and equipment serving the power plant of SVP with GTD [Gas Turbine Engines]	350
17.1 The engine air-supply system	---
17.2 The gas-discharge equipment (GVU) for GTD on SVP	362
17.3 Noise suppressing equipment for a gas turbine power plant	363
18. Designing propulsors for amphibious SVP	---
18.1 Air propellers	364
18.2 Air-jet propulsors (propulsor-ventilators)	371
19. Determining the characteristics of SVP lifting systems	372
19.1 Determining the forced air system characteristics	373
19.2 Calculating air duct resistance	382
20. Peculiarities of the design of the power plant of an SVP with skegs	383

FOR OFFICIAL USE ONLY

	Page
Chapter VII. The selection of the means of maneuvering and control of SVP and providing for stability of motion	386
21. SVP maneuvering qualities	---
21.1 General information on SVP maneuvering qualities	---
21.2 Means providing for SVP directional control	389
21.3 Maneuverability of SVP	392
21.4 The means of directional control and maneuvering adopted on several foreign SVP	394
21.5 Some recommendations on the arrangement of instruments and mechanisms for the control of SVP	396
22. Providing directional control of SVP	397
22.1 Evaluating SVP stability on course	---
22.2 The turning ability of SVP	405
23. Providing dynamic stability in the spatial motion of SVP	411
23.1 The drawing in under the hull of the flexible enclosure	412
23.2 The behavior of the rigid hull when being buried in the sea	415
23.3 The capsizing of SVP	416
Appendices to Part I.	
Appendix I. The principal characteristics of domestic SPK	420
Appendix II. The principal characteristics of foreign SPK and KPK [Military Hydrofoil Ships]	422
Appendix III. Weight, size, seaworthiness, and maneuvering character- istics of SPK	438
Appendix IV. The principal characteristics of the main engines and propulsors of SPK	442
Appendix V. The mechanical properties of structural materials	446
Appendix VI. The general arrangement of domestic and foreign SPK	449
Appendices to Part II.	
Appendix I. The principal characteristics of SVPA	460
Appendix II. The principal characteristics of SVPS	461

COPYRIGHT: Izdatel'stvo "Sudostroyeniye", 1980

9136

CSO: 1861/37

FOR OFFICIAL USE ONLY

FOR OFFICIAL USE ONLY

NUCLEAR ENERGY

UDC 621.039.56

OPERATING AND REPAIRING NUCLEAR POWER STATIONS

Moscow OSOBNOSTI EKSPLOATATSII I REMONTA AES in Russian 1981 (signed to press 11 May 81) pp 2-4, 168

[Annotation, table of contents and introduction from the book "Characteristics of the Operation and Repair of AES's," by Leonid Mikhaylovich Voronin, Energoizdat, 3,500 copies, 168 pages]

[Text] Specific conditions and basic regimes for the operation of AES's with reactors of various types and the technical and economic indicators of AES's are examined. Much attention is paid to radiation safety and to methods for processing and burying the radioactive wastes of AES's, as well as to problems of monitoring the working order of the equipment and the condition of the metal of pipelines and of the basic equipment during operation. The basic requirements for the manipulability of AES's and the prerequisites for providing for reliable and stable AES operation within power-engineering systems are set forth, along with the main problems of organizing and carrying out equipment repairs at AES's and questions of deactivating equipment and of mechanizing repair operations. This publication is a sequel to the book, "Osobennosti proyektirovaniya i skoruzheniya AES" [Characteristics of the Design and Erection of AES's] (Moscow, Atomizdat, 1980).

For specialists who are working in the areas of the design, construction and operation of AES's. Can be used by students of power-engineering and engineering-physics faculties where courses in the design, construction, assembly, tuneup and operation of AES's are being studied.

Table of Contents	Page
Introduction.....	3
Chapter 1. The Operation of an AES.....	5
1.1. Specific prerequisites for the operation of an AES.....	5
1.2. An AES's main operating regimes.....	7
1.3. Characteristics of AES operation associated with the fuel cycle and the need to recharge the reactors with nuclear fuel.....	47
1.4. Basic tasks and methods for providing for reliable and safe operation of AES's.....	53
1.5. The treatment of radioactive wastes during AES operation.....	73
1.6. Radiation safety during AES operation.....	83
1.7. The organizational structure for operation of an AES.....	92

FOR OFFICIAL USE ONLY

FOR OFFICIAL USE ONLY

	Page
Chapter 2. The Repair of AES Equipment.....	94
2.1. Characteristics of AES equipment repair.....	94
2.2. The deactivation of equipment at an AES.....	96
2.3. The organization and execution of equipment repair at AES's.....	106
2.4. The supplying of materials and equipment to AES's for equipment repair.....	119
2.5. Problems of the centralization and specialization of repair work at AES's.....	122
2.6. The main directions for raising the effectiveness and quality of repair at AES's.....	125
Chapter 3. The Operation of an AES in a Power-Engineering System.....	129
3.1. The requirements for manipulability of an AES.....	129
3.2. The manipulability characteristics of an AES.....	134
3.3. AES operating regimes in power-engineering systems.....	143
Chapter 4. The Economics of an AES.....	146
4.1. Characteristics of the economics of an AES.....	146
4.2. The technical and economic indicators of an AES.....	149
4.3. Ways to raise the technical and economic indicators of an AES.....	158
Bibliography.....	162
Alphabetical subject index.....	164

Introduction

A new branch of power-engineering--nuclear--has made an enormous leap in its development in a comparatively short time (a little more than a quarter of a century). The electrical power of the First AES, which was started up on 27 June 1954 in Obninsk, Kaluzhskaya Oblast, was about 5,000 kw. At present the installed capacity of the world's nuclear electric-power stations is about 150 million kw. This rapid development of nuclear power was occasioned primarily by the limited nature of fossil-fuel reserves and the unevenness of their distribution about the globe. Moreover, during AES operation, pollution of the air basin with the sulfur compounds and various combustion products that are discharged in large quantities by power stations that operate on fossil fuels is precluded.

"...Today, throughout the whole world, power plants are discharging into the atmosphere annually 200-250 million tons of ash and about 60 million tons of sulfur dioxide. In the long term, prior to the year 2000, these discharges can grow, respectively, to 1.5 billion and 400 million tons. But nuclear power stations do not need oxygen and do not contaminate the atmosphere with ash, sulfur and other combustion products. These are 'cleaner' stations...."*

During the 10th Five-Year Plan a major step was taken toward the construction of AES's. New capacity was introduced at the Kurskaya, Chernobyl'skaya, Lenin-grad, Beloyarskaya, Novovoronezhskaya, Armyanskaya, Rovenskaya and Bilibinskaya AES's. The erection of large power units is in the completion stage at the Smolenskaya, Yuzhno-Ukrainskaya and Kol'skaya AES's.

*Aleksandrov, A. P. "Budushcheye energetiki [Power Engineering of the Future], KOMMUNIST, No 1, 1976.

FOR OFFICIAL USE ONLY

FOR OFFICIAL USE ONLY

At the end of 1980 the total power of the USSR's nuclear power stations had reached 12.5 million kw.

The generation of electricity at AES's is constantly increasing. Thus, in 1980 alone, the country's nuclear power stations produced 73 billion kw-hr of electricity. This is more electricity than was generated at AES's during all the years of the Ninth Five-Year Plan. During the period 1976-1980, more than 230 billion kw-hr were generated at AES's.

During the 10th Five-Year Plan the erection of prototype power units with VVER-1000 and BN-600 reactors was completed. The startup and mastery in 1980 of the V unit with a VVER-1000 reactor at the Novovoronezhskaya AES enabled conversion to the intense construction of a large series of power units with unified VVER-1000 reactors. Experience in the erection and start of the III unit with BN-600 reactor at the Beloyarskaya AES is of enormous significance for the further acceleration of the construction of nuclear power stations with breeder reactors.

Analyses are now being made of reactor installations with BN [breeder] installations with sodium coolant, with a single-unit electricity power of 800,000 and 1.6 million kw.

During the 11th Five-Year Plan, in accordance with 26th CPSU Congress decisions, the pace of introduction of new capacity at AES's will almost double in comparison with the preceding five-year plan. In 1981-1985 new power units will go into operation at the Kalininskaya, Zaporozhskaya, Rovenskaya, Khmel'nitskaya, Yuzhno-Ukrainskaya, Rostovskaya and Balakovskaya AES's with VVER-1000 reactors. New power units with RBMK-1000 reactors will be introduced at the Kurskaya, Smolenskaya, Chernobyl'skaya and other AES's, and also at the Ignalinskaya AES with RBMK-1500 reactors. All this will enable the generation of electricity at AES's to increase still more and to be brought up to at least 15 percent of all the country's generation of electricity by the end of 1985.

In the next few years most AES's will operate at the base-load regime. In this case, the largest possible amount of secondary fuel--plutonium, which is necessary for supporting the fuel cycle for the next stage of development, which will be based on nuclear power stations with breeder reactors--will be turned out.

The nuclear power stations that are operating in the USSR demonstrate reliable and safe operation. However, the increase in their number and their siting in regions of high population density require that society give serious attention to questions of AES safety.

Questions of the reliability and safety of AES operation require paramount attention. AES designs therefore call for a set of protective, localizing and other arrangements and systems for averting major accidents, as well as measures that preclude the release of radioactive substances outside the AES.

The wide construction of AES's requires reliable and, what is very important, economical solution of the problems of processing and the later burial of radioactive wastes.

COPYRIGHT: Energoizdat, 1981

11409
CSO: 1861/44

10

FOR OFFICIAL USE ONLY

FOR OFFICIAL USE ONLY

UDC 621.039.526.001.573

OPTIMIZATION MODELS OF BREEDER REACTORS

Moscow OPTIMIZATSIONNYYE MODELI REAKTOROV NA BYSTRYKH NEYTRONAKH in Russian 1981
(signed to press 28 Jan 81) pp 2, 232

[Annotation and table of contents from the book "Optimization Models of Breeder Reactors," by German Borisovich Usynin, Aleksandr Sergeyevich Karabasov and Vladimir Anatol'yevich Chirkov, Atomizdat, 1,100 copies, 232 pages]

[Text] A mathematical model of a breeder power reactor with sodium coolant is described. The sequence of computations for the reactor's characteristics, beginning with analysis of the fuel element and ending with derivation of in-kind and economic indicators, which can serve as an efficiency function for solving problems of nonlinear programming, is set forth. Computed data that enable engineering evaluations to be made during the development of a breeder reactor are cited.

For specialists engaged in the design of power reactors, students of senior courses, and post-graduate students who are specializing in the area of nuclear power, and also for mathematicians who are interested in applications of the theory of extremal problems.

Table of Contents	Page
Foreword.....	3
Introduction.....	5
Chapter 1. The General Mathematical Model of a Reactor.....	9
1.1. Fundamental design and technological solutions for modern breeder reactors with sodium coolant.....	9
1.2. Status of the development of mathematical models of breeder reactors.	28
1.3. Choice of optimization parameters.....	37
1.4. Choice of system for the model.....	45
Chapter 2. Analysis of the Central Fuel Element and of the Assembly with the Greatest Heat Stress.....	49
2.1. An approximate calculation of fuel-element efficiency.....	49
2.2. Analysis of the geometric characteristics of the TVS [hot-water supply] and the volumetric composition of the operating unit.....	63
2.3. Thermal and hydraulic analysis of the TVS.....	68
Chapter 3. Simulation of a Reactor's Neutron-Physics Characteristics.....	74
3.1. A method of approximate simulation.....	74

FOR OFFICIAL USE ONLY

FOR OFFICIAL USE ONLY

	Page
3.2. Regressive models of physics characteristics.....	86
3.3. The use of small-group methods.....	106
Chapter 4. The Simulation of Devices for Controlling Reactivity.....	110
4.1. Basic principles for choosing control devices.....	110
4.2. Balance of reactivity.....	115
4.3. The simulation of SUZ [safety and control rods] devices.....	121
Chapter 5. The Reactor's Thermal and Electrical Capacity.....	125
5.1. Characteristics of the field of heat release in the core and breed- ing blanket.....	125
5.2. Computation of the reactor's thermal capacity.....	149
5.3. Computation of the installation's KPD [efficiency].....	156
Chapter 6. Optimization Criteria.....	177
6.1. In-kind criteria.....	177
6.2. Economic criteria.....	184
Chapter 7. Some Results of the Use of Mathematical Models of a Reactor with an Oxide Fuel.....	190
7.1. Formulation of a problem for nonlinear programing and methods for solving it.....	190
7.2. The results of the optimization of various criteria.....	201
7.3. The effect of the indeterminacy of the initial data on the optimiza- tion results.....	209
Bibliography.....	222

COPYRIGHT: Atomizdat, 1981

11409

CSO: 1861/40

FOR OFFICIAL USE ONLY

UDC 621.039.58+621.039.7

RADIATION SAFETY IN NUCLEAR POWER ENGINEERING

Moscow RADIATIONNAYA BEZOPASNOST' V ATOMNOY ENERGETIKE in Russian 1981 (signed to press 13 Jan 81) pp 2, 117-118

[Annotation and table of contents from the book "Radiation Safety in Nuclear Power Engineering," by Lev Aleksandrovich Buldakov, Dmitriy Ivanovich Gusev, Nikolay Grigor'yevich Gusev, Viktor Aleksandrovich Knizhnikov, Oleg Anatol'yevich Pavlovskiy and Rita Yakovlevna Sayapina of the Editorial Board of the Deputy USSR Ministry of Public Health, Atomizdat, 5,000 copies, 120 pages]

[Text] The book, which has been prepared by leading specialists under the Editorial Board of the Deputy USSR Minister of Public Health, cites the results of work to provide for radiation safety in nuclear power engineering. The main attention has been devoted to the state system for protecting the health of workers and preserving the external environment, to questions of radiation hygiene, to the creation of systems of sanitation legislation for operation and handling of sources of ionizing radiation, to providing for the radiation safety of personnel at nuclear-industry enterprises, to evaluation of the radiation situation in regions where AES's are sited, to the thermal effluents of AES's, to problems of radiation safety of the population where nuclear power is used for the district heating of cities, and to the problems of the processing and burial of radioactive wastes.

The book is intended for workers who are associated with solving problems of radiation safety during the industrial use of nuclear energy in the national economy.

Table of Contents	Page
Introduction.....	3
Chapter 1. The State System for Protecting the Health of the Population and for Preserving the Environment.....	7
Chapter 2. Problems of Radiation Hygiene for the Populace.....	10
2.1. Radiation hygiene--a new branch of science.....	10
2.2. The radiation situation in the country.....	12
2.3. The biological effects of small doses and their significance in set- ting standards for hygiene.....	18
2.4. Pressing problems of radiation hygiene in nuclear power engineering..	19

FOR OFFICIAL USE ONLY

FOR OFFICIAL USE ONLY

	Page
Chapter 3. The Creation of a System of Sanitary Norms and Rules for the Use of Sources of Ionizing Radiation.....	20
3.1. USSR Norms for Radiation Safety, NRB-76.....	21
3.2. Basic sanitation rules for work with radioactive substances and other sources of ionizing radiation.....	28
3.3. Sanitation Rules for the Design and Operation of AES's, SP-AES-79...	31
Chapter 4. The Provisioning of Radiation Safety for Personnel at Nuclear Power-Engineering Enterprises.....	37
4.1. Ore-mining enterprises.....	38
4.2. The processing of ores and the manufacture of nuclear fuel.....	40
4.3. Nuclear reactors of AES's.....	43
4.4. Work hygiene during the regeneration of fuel elements and the reuse of nuclear fuel.....	48
Chapter 5. Gas and Aerosol Discharges of AES's and the Radiation Situation in Regions Where They are Sited.....	51
5.1. Reactors as sources of the formation of radionuclides.....	51
5.2. Measures for limiting radioactive discharges into the environment...	53
5.3. Radioactive gas and aerosol discharges from AES's.....	55
5.4. The radiation situation in a region of AES siting caused by radioactive gas and aerosol discharges.....	60
Chapter 6. Radioactive and Thermal Effluents of AES's and the Preservation of Water Bodies from Pollution.....	69
Chapter 7. Nuclear District Heating of Cities and Radiation Safety.....	87
Chapter 8. Radiation Safety During the Processing and Burial of Radioactive Waste.....	95
Chapter 9. Evaluation of the Possible Consequences of Exposure of the Population to Radiation.....	106
Bibliography.....	115

COPYRIGHT: Atomizdat, 1981

11409

CSO: 1861/43

FOR OFFICIAL USE ONLY

FOR OFFICIAL USE ONLY

UDC 621.039.5

PRACTICAL PROBLEMS OF OPERATING NUCLEAR REACTORS

Moscow PRAKTICHESKIYE ZADACHI PO EKSPLOATATSII YADERNYKH REAKTOROV in Russian 1981
(signed to press 24 Mar 81) pp 2, 288

[Annotation and table of contents from the book "Practical Problems in the Operation of Nuclear Reactors," by Vladimir Ivanovich Vladimirov, Energoizdat, 3800 copies, 288 pages, third edition, revised and supplemented]

[Text] Questions of the physics of power reactors from the point of view of their operation are examined. The main attention is devoted to the physical meaning of the processes that accompany reactor operation and that determine a reactor's energy capabilities and manipulability characteristics. Standard procedures are cited, and examples of the solution of practical problems are given, along with problems for independent solution (with answers) and monitoring questions for checking on assimilation of the material. Certain questions on providing for nuclear safety of the reactor and for efficiency of the core, and also on standard procedures for making neutron-physics measurements and refinements of the reactor's characteristics during physical startup and during the operating process, are examined. The first edition of the book was published in 1972, the second in 1976.

For scientists, engineers and technicians who create and operate nuclear power-engineering installations, and also for those who are preparing for this work.

Table of Contents	Page
Introduction.....	3
Basic Abbreviations.....	7
Chapter 1. The Nuclear Reactor as a Source of Energy and Ionizing Radiation	8
1.1. The atom. The atomic nucleus. Atomic energy.....	8
1.2. The chain reaction. The multiplication factor. Reactivity.....	15
1.3. The reactor's power. Energy release in the core.....	22
1.4. The reactor's ionizing radiation.....	29
Chapter 2. The Physical Processes That Accompany the Reactor's Operation...	43
2.1. Burn-up and slagging of the fuel.....	43
2.2. Fuel breeding.....	49
2.3. Steady-state xenon poisoning of the reactor.....	52
2.4. Nonsteady-state xenon poisoning.....	61
2.5. Steady-state samarium poisoning of the reactor.....	93
2.6. Nonsteady-state samarium poisoning.....	97

FOR OFFICIAL USE ONLY

FOR OFFICIAL USE ONLY

	Page
2.7. The temperature effect.....	107
2.8. Reactor life.....	115
Chapter 3. Control of the Nuclear Reactor.....	128
3.1. The parameters that determine the reactor's capacity and the speed of change in capacity.....	128
3.2. Subcritical and critical states of the reactor.....	129
3.3. Supercritical state of the reactor.....	140
3.4. Devices for reactor regulation.....	149
3.5. Startup of the reactor, heat-up and operation at the power level of the capacity.....	169
3.6. Stopping and shutdown cooling of the reactor.....	182
Chapter 4. Nuclear Safety of the Reactor and the Thermal-Engineering Relia- bility of the Core.....	194
4.1. Characteristics of the nuclear reactor as an energy source.....	194
4.2. The provisioning of nuclear safety for the reactor.....	197
4.3. The provisioning for the thermal-engineering reliability of the core.....	216
Chapter 5. Neutron-Physics Measurements During Reactor Operation.....	223
5.1. The necessity for and the amount of neutron-physics measurements (NFI).....	223
5.2. Determination of the critical charge.....	224
5.3. Calibration of the regulating devices.....	229
5.4. The plotting of differential and integral characteristics.....	240
5.5. The determination of temperature and power effects and the coeffi- cient of reactivity.....	245
5.6. Determination of steady-state and nonsteady-state xenon poisoning of the reactor.....	248
5.7. Refinement of the power-generation curve.....	251
5.8. Determination of the distribution of energy release.....	252
5.9. Refinement of the physical characteristics of the regulating devices.....	254
Monitoring Questions and Problems for Independent Solution.....	256
Answers to the Monitoring Questions and Problems for Independent Solution...	267
Appendices.....	271
Bibliography.....	287

COPYRIGHT: Atomizdat, 1976 Energoizdat, 1981

11409

CSO: 1861/41

FOR OFFICIAL USE ONLY

UDC 533.92;621.039.61

CALCULATING COMPRESSION OF DT-MIXTURE BY ELECTRICALLY IMPLoded CYLINDRICAL SHELL

Novosibirsk ZHURNAL PRIKLADNOY MEKHANIKI I TEKHNIChESKOY FIZIKI in Russian No 6, Nov-Dec 80 (manuscript received 8 Oct 79) pp 3-10

[Article by V. I. Afonin, Yu. D. Bakulin and A. V. Luchinskiy, Chelyabinsk, Tomsk]

[Text] One way to solve the problem of controlled nuclear fusion is to heat a target containing a DT mixture as it is compressed by a dense shell accelerated to velocities of the order of 10^7 cm/s or more [Ref. 1]. One of the ways to do this is by using megagauss magnetic fields [Ref. 2]. An attractive feature of this technique is the capability of getting a comparatively high ($\geq 1\%$) coefficient of transfer of initially stored energy to the shell. In this process, kinetic energy is picked up both due to magnetic field pressure, and due to dispersal of matter from the surface of the shell. Both mechanisms of acceleration operate in electric implosion of the shell by an intense current pulse. Ref. 3 gives the calculation of electric implosion of a thin cylindrical shell when a megajoule capacitor bank is discharged across it. The calculation yields compression rates of up to $3 \cdot 10^7$ cm/s; however, because of the comparatively slow rates of increase in current provided by capacitor banks, it is necessary to take a very low initial relative thickness of the shell of $\sim 10^{-5}$. The heating of the gas filling the shell and the conditions of the fusion reactions were not considered in Ref. 3.

Ref. 4 gives the results of numerical calculation of compression and thermonuclear ignition of a DT mixture as it is compressed by a cylindrical shell. It is found in the calculations that combustion of deuterium-tritium with positive energy yield is possible when a constant power of $\geq 3 \cdot 10^{14}$ W is released in the shell. Although it is pointed out that an electrodynamic method can be used for releasing such power, the matter is not pursued further, nor are magnetohydrodynamic effects in the shell and plasma considered.

Our paper is an attempt at a computational evaluation of feasibility of attaining nuclear fusion by electric implosion of a shell. Consideration is taken of processes in the electric circuit of the facility, magnetohydrodynamic processes in the target, and the course of fusion reactions. Compression of the shell is taken as ideally symmetric. Problems of the stability of compression [Ref. 5] are not considered in this paper.

An analysis was made in Ref. 6 of electrophysical facilities from the standpoint of their capabilities for setting up energy densities of the order of megajoules

FOR OFFICIAL USE ONLY

FOR OFFICIAL USE ONLY

per gram in a wire upon electric explosion. It was shown that such a capability can be realized if lines connected in parallel with distributed parameters are discharged into a load in the shape of a cylindrical shell. Therefore in the following we will limit ourselves to consideration of electric explosion of copper cylindrical shells located in the center of a disk collector to which a system of lines is connected in parallel.

To describe electric explosion of a cylindrical shell, we have used a system of one-dimensional equations of magnetogasdynamics (MGD) with thermal conductivity, where the latter is accounted for in the diffusion approximation. The coefficient of thermal conductivity was taken as proportional to the $5/2$ power of temperature, i. e. it was assumed that heat is transferred by electrons. If there was gas inside the shell, the energy of bremsstrahlung arising upon compression of this gas did not return to the shell, but was extracted from the load by the appropriate heat sink function. The energy of alpha particles of thermonuclear origin absorbed in the gas was also disregarded.

As in Ref. 7 in calculations of processes in copper, we used an interpolation equation of state [Ref. 8] describing the vaporization of copper and the region of the vapor-liquid mixture. The way that electrical conductivity of copper depends on density and thermal energy was also described as in Ref. 7. In the temperature region up to a few electron-volts and at densities greater than 0.1 g/cm^3 , the electrical conductivity was selected on the basis of experiments on electric explosion of wires. In the region of densities lower than 0.01 g/cm^3 and temperatures of $10\text{--}100 \text{ eV}$, the data on electrical conductivity were taken from Ref. 9, where they were calculated from the Saha and Boltzmann equations with consideration of shielding. In a certain region of states of copper, electric conductivity was interpolated between calculated experimental values and data of Ref. 9, and in isolated cases was even extrapolated to temperatures greater than those considered in Ref. 9. Naturally, the accuracy of interpolation and extrapolation requires experimental verification. However, calculations show that such states of copper are reached only in the last phases of compression, and errors in the description of electrical conductivity even by two orders of magnitude do not cause any appreciable change in the compression process. The equation of state of an ideal gas with $\gamma = 5/3$ was used in calculating gases of D_2 or DT enclosed in a shell. On the other hand, if the DT mixture was frozen, it was taken into consideration with the following equation of state:

$$p = p_x + p_r = \frac{\rho_0 c_0^2}{n} (\delta^n - 1) + \Gamma \rho_0 \delta \epsilon_r,$$

$$\epsilon = \epsilon_x + \epsilon_r, \quad \epsilon_x = - \int_{v_0}^v p_x dv,$$

$$n = \begin{cases} n_1, & \text{if } \delta < \delta_1, \\ n_2, & \text{if } \delta_1 \leq \delta \leq \delta_2, \\ 5/3, & \text{if } \delta > \delta_2, \end{cases} \quad \Gamma = \begin{cases} \left(1 - \frac{\epsilon_r}{Q}\right) \Gamma_H + \frac{2}{3} \frac{\epsilon_r}{Q}, & \text{if } \epsilon_r < Q, \\ 2.3, & \text{if } \epsilon_r \geq Q, \end{cases}$$

where ρ_0 and c_0 are the initial density and speed of sound, δ is relative density, p is pressure, ϵ is specific energy density, v is specific volume. In accordance with the experimental data given in Ref. 10, the constants in this equation of state were taken as equal to the following quantities:

FOR OFFICIAL USE ONLY

FOR OFFICIAL USE ONLY

$$\rho_0 = 0.2 \text{ g/cm}^3, c_0 = 1.73 \text{ km/s}, n_1 = 3, n_2 = 2, \\ \delta_1 = 10, \delta_2 = 100, \Gamma_H = 2/3, Q = 0.27 \text{ kJ/g}.$$

The gas compressed inside the shell was taken as conductive. In this assumption, consideration was taken of heating of the gas both due to the work done by the shell, and due to joule heat released during passage of current. The electrical conductivity of the gas was determined from formulas of electrical conductivity of completely ionized hydrogen plasma from Ref. 11. The possibility of arisal of individual channels of electric breakdown was disregarded in the calculations.

The system of MGD equations for calculating the load was solved on a computer together with the system of equations of the electric circuit. Line length and storage of energy in the lines were determined after completing calculation of the process based on its time. The collector of the facility was treated as a disk line with wave impedance depending on radius.

If the time of wave propagation through the collector is much less than the time of wave propagation through the main lines, then the current in the line-collector-load system (at constant load resistance R_L) varies exponentially from a value of $U_0/(R_C + R_L)$ to $U_0/(R_L + R_0)$, where U_0 is the voltage to which the lines are charged, R_0 is the wave impedance of the coaxial line system, R_C is the circuit resistance, i. e. the sum of R_0 and the collector resistance. Therefore a fairly good approximation of the equivalent circuit of the facility is that shown in Fig. 1, where R_{eq} is taken as

$$R_{eq} = R_0 + (R_C - R_0)e^{-1/\tau},$$

where τ is the time of wave passage through the collector.

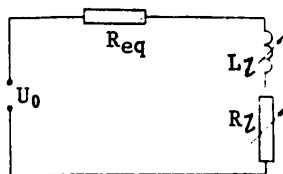


Fig. 1

A series of calculations has confirmed the validity of the relations derived in Ref. 6. MGD calculations showed that dependence of the rate of acceleration of the imploding copper shell and the energy input on voltage U_0 is comparatively weak. With an increase in U_0 from 0.75 to 2 MV, there is a slight reduction in the time of collapse of the shell and an increase in energy input. A further increase in U_0 has practically no effect on these quantities, but apparently should lead to complication of the construction of the facility. A reduction of R_0 increases the rate of current rise in the load, and hence also increases the rate of energy input. The latter is a decisive factor in achieving nuclear fusion. Unfortunately there is a limit below which no change in R_0 can increase the rate of energy input. This limit is the load resistance R_L that begins to determine

FOR OFFICIAL USE ONLY

FOR OFFICIAL USE ONLY

the rate of energy input to the conductor at $R_0 < R_L$. Nor does it make any sense to reduce R_0 below R_L from the standpoint of energy expenditures, since the energy stored in the lines at fixed U_0 and process time θ is inversely proportional to R_0 , and the process of energy input is determined by the quantity R_L .

R_L can be reduced only by either reducing the length of the cylindrical conductor, or by increasing its radius. Of particular significance for the process is an increase in the radius of the shell. Such an increase leads to an increase in acceleration (due to an increase in the rate of current rise) as the shell is accelerated by the magnetic field;

to an increase in the base of acceleration of the shell (as mass remains constant); to an abrupt increase in the maximum velocity of dispersal of the shell (due to the first two factors); to a reduction of heat losses in the gas (due to a reduction in the time of compression). The aggregate of these factors produces a sharply nonlinear rise of maximum temperature of the compressed gas with increasing radius and decreasing relative thickness of the copper shell.

The calculations showed that with other parameters fixed, the maximum temperature of the compressed gas is most significantly dependent on its initial density ρ_0 . To get temperatures in the gas of the order of several keV necessary for the beginning of a thermonuclear reaction, the conductor must be filled with gas at pressure of the order of atmospheric or less, i. e. $\rho_0 \leq 0.0002$. An increase in ρ_0 by two orders of magnitude led to nearly cold compression of the gas.

The results of calculations show that the length of the lines can be taken such that the double time of wave transmission through the lines is somewhat less than the time of shell compression. In this case, the second part (in time) of the process takes place with somewhat lower voltage across the lines, but this has little effect on the final result since most of the energy consumed by the load is already in its magnetic field.

These research calculations were not intended to optimize the load on any given facility. The main purpose of the calculations was to determine the laws governing the process of compression of matter in electric implosion of a cylindrical shell, and to demonstrate the feasibility of this method from the standpoint of achieving nuclear fusion. Several variants of calculations of various systems are given below.

Variant 1. A copper shell with length of 1 cm and thickness of 0.01 cm and with outside radius of $r_H = 1.25$ cm is filled with a gaseous DT mixture with initial density $\rho_0 = 3 \cdot 10^{-5}$ g/cm³. The shell is connected through a collector to a system of lines charged to $U_0 = 2$ MV with total wave impedance of $R_0 = 0.005 \Omega$.

Preliminary calculation showed that maximum compression of the gas occurs at $t = 0.33 \mu s$. On this basis, the length of the lines was taken as equal to 280 cm, which corresponds to energy storage of 34 MJ. At time $t = 0.17 \mu s$, the voltage across the lines had fallen to 1.8 MV. The calculation showed that the maximum velocity of the shell was reached at its inside boundary, being 20 cm/ μs . Fig. 2 shows graphs of the time dependence of the inside radius of the shell r_b and the average gas temperature T_c . Profiles of temperature T and density ρ in the shell

FOR OFFICIAL USE ONLY

FOR OFFICIAL USE ONLY

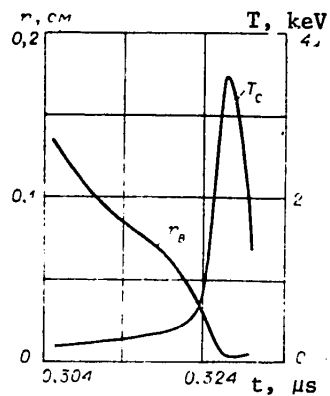


Fig. 2

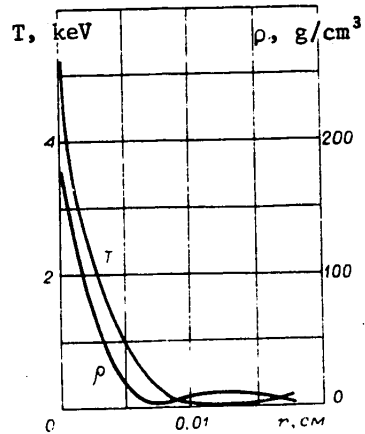


Fig. 3

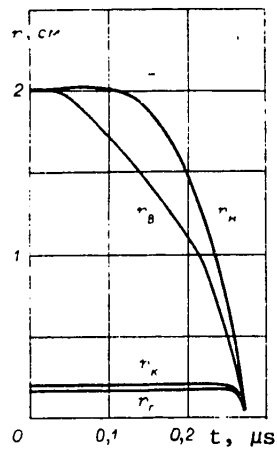


Fig. 4

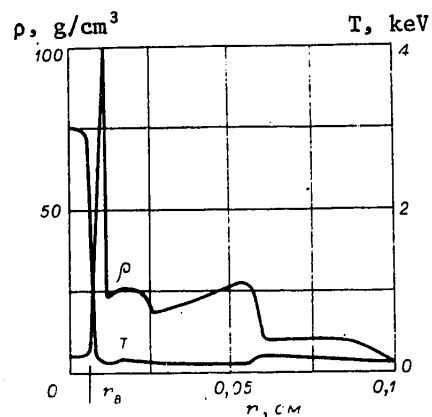


Fig. 5

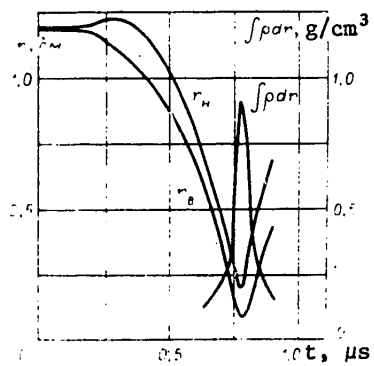


Fig. 6

FOR OFFICIAL USE ONLY

FOR OFFICIAL USE ONLY

and gas system as shown in Fig. 3 refer to the instant near the time of maximum gas compression. Temperature and density are nearly constant in the gas. Since the thermal conductivity in copper falls sharply with increasing density, the high density peak near the inside boundary of the copper abruptly reduces the heat transfer from the gas. This explains the rapid drop in temperature in the narrow layer of copper adjacent to the boundary. The quantity r_B on Fig. 2 denotes the position of the interface between gas and shell.

The energy transferred to the shell and gas was 10 and 0.06 MJ respectively. Maximum energy in the shell was 20 MJ/g. The neutron yield of the system was $6 \cdot 10^{17}$ neutrons, and the energy of the alpha particles absorbed in the gas was three times the energy of the gas transferred to it by the shell. However, we cannot expect any intense thermonuclear flare here [see Ref. 12] as the maximum $\int \rho dr$ in the gas was 0.03 g/cm^2 .

Variant 2. The mass is reduced in the copper shell as compared with variant 1. Its outside radius is increased to 2 cm with shell thickness of 0.001 cm, and the length of the shell remains 1 cm. Inside the shell to a radius of 0.17 is DT gas with density of 10^{-4} g/cm^3 , surrounded by a frozen layer of DT ($0.17 \leq r \leq 0.2$) with density of 0.2 g/cm^3 . Between this layer and the shell is a gap filled with gas of low density $\rho = 2 \cdot 10^{-6} \text{ g/cm}^3$. The voltage across the lines was taken as 2 MV and the wave impedance of the lines was $R_0 = 0.0075 \Omega$. At time $t = 0.135 \mu\text{s}$ the voltage had fallen to 1.71 MV.

Fig. 4 shows time dependences of the outside r_H and inside r_B radii of the shell, and also of the outside r_K and inside r_r radii of the frozen DT layer. After impact of the shell along the DT layer, the velocity of their interface was $37 \text{ cm}/\mu\text{s}$, and the inner surface of the layer was accelerated to $42 \text{ cm}/\mu\text{s}$. Within 3 ns after impact the gas is compressed to $r_r = 4.3 \cdot 10^{-5} \text{ cm}$, and its average temperature rises to 8.5 keV. A little previous to this instant the temperature and density in the DT layer have the profiles shown in Fig. 5. We note that within 0.4 ns the DT layer is compressed, the profiles in the layer are equalized, and the average values of temperature and density are 0.6 keV and 40 g/cm^3 . Of the 21 MJ originally stored in the lines, 7 and 1 MJ respectively are transferred to the shell and the DT. The maximum values of the internal energy in the copper close to its inner boundary reach 70 MJ/g. The energy of the alpha particles absorbed in the gas was 7 times the energy from compression of the gas by the shell, the quantity $\int \rho dr$ was 0.4 g/cm^3 and the neutron yield was of the order of 10^{17} , half of this amount falling to the DT gas, and the other half to the initially frozen DT layer.

Variant 3. DT gas with density $\rho_0 = 0.07 \text{ g/cm}^3$ is enclosed in a copper cylindrical shell 0.012 cm thick with outside radius $r_H = 1.2 \text{ cm}$. Length of the shell is 3 cm. A system of lines with voltage $U_0 = 2 \text{ MV}$ and wave impedance $R_0 = 0.03 \Omega$ is discharged across the shell. The problem was considered to ascertain the consequences of compressing a gas of high initial density.

The compression process took place comparatively slowly: rate of dispersal of the shell did not exceed $4 \text{ cm}/\mu\text{s}$. Maximum compression was only 220. The gas was practically unheated. By the instant of maximum compression the gas was a thin column of high-density cold matter. The quantity $\int \rho dr$ rose to 0.92 g/cm^2 . Shown on Fig. 6 are graphs of the time dependence of the outer r_H and inner r_B radii

FOR OFFICIAL USE ONLY

of the shell and the quantity $\int \rho \, dr$. Calculation shows that of the 26 MJ of initial energy, 21 MJ is transferred to the shell+gas system. Of this energy, 4.2 MJ make up the energy of the shell, 3.5 MJ comprise the energy of the gas, and the remainder is in the magnetic field of the system. It should be noted that the required initial energy store in the lines is appreciably dependent on the maximum value of $\int \rho \, dr$. For example, only 12 MJ of the initial energy store is needed to get a value of 0.67 for this quantity.

One thing that all calculations have in common is that when the impedances of the load and lines are sufficiently well matched, a large percentage of the energy stored in the lines is transferred to the load and its magnetic field. In calculation of one system with energy store of 2.5 MJ, this fraction came to more than 90%, the load energy proper exceeding 30% of this store. Let us note that for this system we cannot expect self-heating of the gas due to a thermonuclear reaction; however, the neutron yield found in the reaction was rather high: $\sim 10^{15}$.

It is interesting to note a characteristic feature of gas compression with electric implosion of a shell that is associated with the change in distribution of conductivity in the conductor during the process of electric implosion. In the initial stage, due to the skin effect the maximum current density falls to the region of the conductor that is adjacent to its outside boundary. The magnetic field prevents outward dispersal of the conductor; however, a slight density reduction and the contribution of joule heat still result in a drop in conductivity of the outer part of the conductor by about two orders of magnitude. This intensifies the process of penetration of the magnetic field and maximum current density into the conductor. The magnetic field approaches the inner boundary of the copper shell with a large gradient. A rapid rise in magnetic and hydrodynamic pressures (due to high current density and release of joule heat) causes abrupt acceleration and load relief of the inside part of the shell. The gas with low density and pressure located inside the shell does not hold back this pressure. As the density of the inner part of the conductor drops, its conductivity decreases and becomes minimum (with respect to the cross section). The current density curve drops sharply with decreasing radius. Contributing to this behavior is the distribution of density (and accordingly of conductivity) that is set up in the shell, falling off from the outer boundary toward the inner boundary. From about this moment, the inner layers of the shell continue to travel by inertia, while the outer layers, and gradually the entire mass of the shell begin to be accelerated by the magnetic field. This process continues until the inner layers begin to decelerate due to resistance of the compressed gas. After this, the densities are equalized, and consequently so are the conductivity and density of the gas over the cross section of the conductor. The current density gradient remains high only in a narrow neighborhood of the inside boundary of the conductor. This produces an additional impact on the gas near the instant of maximum compression. This is illustrated by Fig. 2, where we can see that the inside radius of the shell acquires additional inward acceleration near the instant when it stops.

Let us say a few words about the effect that the current passing through the gas has on the process of compression of the gas by the shell. The behavior of the process in all calculations was the same. Appreciable conductivity in the gas was noted at times close to the instant of maximum compression of the gas, when its temperature rose to a value of 1 keV. As the gas was further compressed,

FOR OFFICIAL USE ONLY

its conductivity increased rapidly, becoming several orders of magnitude greater than that of copper. Current began to flow through the gas, but despite the difference in conductivities of the materials pointed out above, the current density in the gas was comparable with the densities of current flowing in the copper because of the small radii, and hence the large inductive reactance. And since the cross sectional area of the gas at these instants was several orders of magnitude less than the cross sectional area of the copper, nearly all the current went through the copper conductor. The difference of maximum temperature reached in the gas with and without consideration of conductivity was no more than a few percent.

The efficiency of these installations may be comparatively high. For example in variant 2 a comparatively small fraction of the DT (about 1%) needs to be reacted to get an overall efficiency greater than unity (with respect to the initial energy store in the lines).

Assumptions to simplify calculations are: one-dimensional approximation, consideration of heat conduction in the diffusion approximation, one-temperature plasma, and some others that idealize the described results. Therefore the calculations only illustrate the maximum capabilities of these systems. More complete consideration of the physical phenomena that occur in electric implosion of cylindrical shells may make considerable corrections both in the results of the calculations and in the choice of parameters of the systems. However, the calculated results and data published in Ref. 1-5 show the advisability of further research on compression processes in electric implosion of cylindrical shells.

REFERENCES

1. Linhart, J. G., "Very-High-Density Plasmas for Thermonuclear Fusion", NUCLEAR FUSION, Vol 10, No 3, 1970.
2. Linhart, J. G., "Rocket-Driven Liners for Fusion Triggers and for Very-High-Density Reactors", NUCLEAR FUSION, Vol 13, No 3, 1973.
3. Turchi, P. J., Baker, W. L., "Generation of High-Energy Plasmas by Electromagnetic Implosion", APPLIED PHYSICS, Vol 44, No 11, 1973.
4. Varnum, W. S., "Electrically Imploded Cylindrical Fusion Targets", NUCLEAR FUSION, Vol 15, No 6, 1975.
5. Harris, E. G., "Rayleigh-Taylor Instabilities of a Collapsing Cylindrical Shell in a Magnetic Field", PHYSICS OF FLUIDS, Vol 5, No 9, 1962.
6. Bakulin, Yu. D., Luchinskiy, A. V., "Estimates of Feasibility of Getting High Energy Densities in Electric Implosion of Cylindrical Shells", ZHURNAL PRIKLADNOY MEKHANIKI I TEKHNICHESKOY FIZIKI, No 1, 1980.
7. Bakulin, Yu. D., Kuropatenko, V. F., Luchinskiy, A. V., "Magnetohydrodynamic Calculation of Exploding Wires", ZHURNAL TEKHNICHESKOY FIZIKI, Vol 46, No 9, 1976.
8. Kuropatenko, V. F., Nechay, V. Z., Sapozhnikov, A. T., Sevast'yanov, V. Ye., "Doklad na Vsesoyuznom seminare po modelyam mekhaniki sploshnoy sredy" [Report

FOR OFFICIAL USE ONLY

FOR OFFICIAL USE ONLY

to the All-Union Symposium on Models for Mechanics of Continuous Media],
Novosibirsk, 1973.

9. Kalitkin, M. N., Kuz'mina, L.V., Rogov, V. S., "Tablitsy termodinamicheskikh funktsiy i transportnykh koefitsiyentov plazmy" [Tables of Thermodynamic Functions and Plasma Transport Coefficients], Institute of Problems of Mechanics, USSR Academy of Sciences, 1972.
10. Grigor'yev, F. V., Kormer, S. B., Mikhaylova, O. L., Tolochko, A. P., Uralin, V. D., "Equation of State of Molecular Phase of Hydrogen in Solid and Liquid States at High Pressure", ZHURNAL EKSPERIMENTAL'NOY I TEORETICHESKOY FIZIKI, Vol 69, No 2(8), 1975.
11. Braginskiy, S. I., "Voprosy teorii plazmy" [Problems of Plasma Theory], Gosatomizdat, 1963.
12. Mason, R. J., Morse, R. I., "Tamped Thermonuclear Burn of DT Microspheres", NUCLEAR FUSION, Vol 15, No 5, 1975.

COPYRIGHT: Izdatel'stvo "Nauka", "Zhurnal prikladnoy mekhaniki i tekhnicheskoy fiziki", 1980

6610

CSO: 8144/0238

FOR OFFICIAL USE ONLY

FOR OFFICIAL USE ONLY

NON-NUCLEAR ENERGY

DEVELOPMENT OF TURBOGENERATOR CONSTRUCTION IN USSR

Kiev TEKHNIЧЕСКАЯ ЭЛЕКТРОДИНАМИКА in Russian No 6, Nov-Dec 80 (manuscript received 11 Aug 80) pp 29-38

[Article by Ya. B. Danilevich, doctor of technical sciences, deputy director of All-Union Scientific Research Institute of Electric Machine Construction, Leningrad]

[Text] In 1920 with proclamation of the GOELRO Plan [Gosudarstvennaya komissiya po elektrifikatsii Rossii; State Commission on Electrification of Russia], our nation was producing 500 million kWh of electric energy per year. In 1979 we produced 1200 billion kWh, i. e. 2400 times as much.

About 75% of our electric energy is produced in fossil-fuel plants. In the ensuing years we have built such large GRES's as those in Zaporozh'ye, Uglegorsk and elsewhere.

Development of nuclear power has advanced considerably in recent years. Powerful AES's have been built: Beloyarsk, Novo-Voronezhsk, Kursk, Leningrad and so on.

Keeping pace with the development of fossil-fuel and nuclear electric plants has been the development of Soviet turbogenerator construction. The power of the first Soviet turbogenerator was 500 kW. At the present time the first turbogenerator set with power of 1200 MW and speed of 3000 rpm has been put on-line at the Kostroma GRES, and the Elektrosila Plant has tested the first 1000 MW, 1500 rpm turbogenerator for an AES.

The development of turbogenerator construction is directly related to the largest electric machine building plants of Leningrad Industrial Power Association: Elektrosila, Elektrot'yazhmash and Sibelektrot'yazhmash, and to the leading scientific research centers: the All-Union Scientific Research Institute of Electrical Machine Building, the Scientific Research Institute of the Elektrot'yazhmash Plant, the Scientific Research Institute of the Sibelektrot'yazhmash Plant, and the Institute of Electric Motors, UkSSR Academy of Sciences.

Let us examine the principal stages of development of turbogenerator construction.

Prewar Stage of Development. Preparation for turbogenerator production was started in 1923 at the Elektrosila Plant. The first turbogenerators with power of 500-3000 kW were made in accordance with blueprints of the Vol'ta Plant that were transferred to the Elektrosila Plant during World War I. Ten turbogenerators of this type were built in 1924 with total power of about 12,000 kW.

FOR OFFICIAL USE ONLY

FOR OFFICIAL USE ONLY

From 1924 through 1928 production was mastered on a series of turbogenerators including 14 types of machines with power from 300 to 16,000 kW. In 1929 this series was updated with a reduction in number of types to 9, the power range of the machines being from 500 to 24,000 kW. Structural components were welded rather than cast in the new series, and the bearings were improved. The rotors and banding rings were ordered from abroad. Class A insulation was used for the rotor windings with the exception of machines with power of 24,000 kW. Active steel sheets were paper-insulated. The stator winding in the groove section was insulated by a micanite sleeve, the end sections of the windings were evolute, turned back at an angle of 90° and insulated by varnished strips. A tangential-radial (pocket) cooling system was used for the stator, while an axial cooling system with subslot channels was used for the rotor. Air circulation in the machine was provided by squirrel-cage blowers on the rotor, the ventilation system was closed with the use of air coolers.

A great advance in the thirties was mastery of four-pole turbogenerators of 50,000 kW power with introduction of new technological processes at the Elektrosila Plant [Ref. 10].

Stator winding insulation was continuous, impregnated, made from micatape. Impregnation was with asphalt under pressure in special impregnating autoclaves. The end sections began to take the shape of a tapered basket, appreciably reducing the additional short-circuit losses; nonmagnetic stator pressure plates were first used for the same purpose.

The rotor winding had class B insulation. The insulation in the slotted section was made in the form of a micanite sleeve; the end sections were insulated by micatape and asbestos tape; aluminum saddles were placed over the insulated end sections.

The turbogenerator had a radial multi-jet cooling system with all cooling air blown through the gap.

In 1938, the Khar'kov Turbogenerator Plant made the first turbogenerator (four-pole) with power of 100,000 kW. This unit had a compound (three-piece) rotor with mass of 100 metric tons. This turbogenerator is even now in successful operation at the Zuyevskaya GRES.

The development of Soviet turbogenerator construction subsequently has taken the road of two-pole turbogenerator construction.

In 1937 the Elektrosila Plant developed a new series of T2 turbogenerators with power from 750 kW to 100,000 kW.

A turbogenerator with power of 100,000 kW was made in 1937 for the Novomoskovsk GRES. The mass of the rotor forging was about 50 metric tons. The forging was made from an ingot with mass of 150 metric tons. The yield stress of the material was 55 kg/mm², relative longitudinal extension was more than 16%. The generator was cooled by four free-standing blowers. The rotor had surface cooling.

Turbogenerator Construction in the Forties and Fifties. In 1946 the Elektrosila Plant made the first hydrogen-cooled turbogenerator with power of 100,000 kW. The generator had the same geometry of active sections as the air-cooled turbogenerator.

FOR OFFICIAL USE ONLY

The housing of the machine was made gas-tight and strong, and the machine was equipped with hydrogen cooling units. According to test data, generator efficiency was raised by 1%.

The next stage in development of turbogenerator construction was a 150,000 kW hydrogen-cooled turbogenerator made in 1957. This unit now took full advantage of hydrogen cooling. The turbogenerator was built for a voltage of 18 kV and power factor of 0.9 with excess hydrogen pressure of 0.7 atm. The rotor diameter was 1075 mm, and the yield stress of the material was increased to 60 kg/mm². Nonmagnetic steel with yield stress of 90 kg/mm² was used for the banding rings of the rotor. Axial blowers were used, situated to either side of the rotor barrel. The rotor was cooled from the outside of the barrel, and in addition the gas was fed beneath the end sections of the rotor winding. The stator was cooled by a multi-jet radial arrangement. For cooling the gas, eight gas coolers were provided, installed vertically in sets of four on each side. This 150,000 kW turbogenerator was the largest in Europe at that time, and was at the limit of overall dimensions.

In 1954, turbogenerator construction was transferred from the Khar'kov Turbogenerator Plant to the State Union Plant of Diesel-Locomotive Electric Equipment, today's Elektrot'yazhmash Plant imeni V. I. Lenin. In 1955 the Elektrot'yazhmash Plant worked out an original design for type TGV-25 turbogenerator with indirect hydrogen cooling at a hydrogen pressure of 0.03 atm. This design used welded stator shields with built-in bearings, a disk hydrogen seal with low oil flowrate, vertical placement of the gas coolers, fan coolers on the shaft, and cantilevered rotor banding rings.

In 1956, on the basis of the TGV-25 turbogenerator, the first TVS-30 turbogenerator was built with power of 30,000 kW with hydrogen cooling at pressure of 0.03-0.5 atm. Weight was lower and heating of the end sections of the rotor winding was reduced as compared with the TGV-25 turbogenerator.

Turbogenerators With Power of 200,000 and 300,000 kW. At the same time that turbogenerators with indirect hydrogen cooling were being produced at the Elektrosila and Elektrot'yazhmash plants in 1954-1957, considerable research was being done to develop new cooling systems.

At the Elektrosila Plant, based on research that had been done, a system was developed for direct cooling of the rotor winding by hydrogen drawn from the gap between rotor and stator.

At the Elektrot'yazhmash Plant, the TVO-30 turbogenerator with power of 30,000 kW, voltage of 10.5 kV was developed, manufactured and tested. This turbogenerator used direct hydrogen cooling of the stator and rotor windings at a hydrogen pressure of 3 atm. The stator core had an axial ventilation system. A compressor was used to develop the necessary hydrogen head. An oil end seal for the shaft was used for the first time with piston rings between the yoke and the insert of the seal.

In 1957, on the basis of research that had been done, the Elektrosila Plant started making 200,000 kW turbogenerators type TVF-200 with voltage of 11 kV using indirect hydrogen cooling of the stator winding and direct cooling of the rotor winding with hydrogen drawn off from the gap. An original multi-jet hydrogen cooling system with improved technological properties was used for cooling the rotor winding. An advantage of the system is the comparatively low nonuniformity of heating of

FOR OFFICIAL USE ONLY

the winding with respect to the length of the rotor. Besides, this system does not require high gas pressures, and therefore ordinary axial fans can be used that ensure overall circulation of the gas in the machine. Lengthwise of the rotor, sections with input orifices on the surface of the active part alternate with sections of output orifices, providing the multiple jets in the system. The end sections of the winding are cooled by gas that flows through internal channels milled in the turns of the winding. The winding and core of the stator are cooled by hydrogen circulating through radial channels in the core and in the zone of the end sections of the winding. The stator is cooled by a three-jet radial system. The sectioning of the rotor is matched to the stator ventilation arrangement.

After making two TVF-200 turbogenerators, it was deemed advisable to use water-cooled stator windings for 200,000 kW machines. Therefore the TVF series was subsequently retained for powers of 60,000 and 100,000 kW.

The construction and technology for manufacturing water-cooled windings were studied on an experimental 30,000 kW turbogenerator. Tests of the machine showed high efficiency of the system, and therefore it was used for turbogenerators of 150,000 kW or more.

The first turbogenerator of the TVV series with power of 150,000 kW and voltage of 18 kV with water-cooled stator winding and direct hydrogen cooling of the rotor winding was made by the Elektrosila Plant in 1959. Subsequently, TVV-200-2 turbogenerators were built with powers of 200,000 kW, 15 and 75 kV, and the TVV-300-2 with power of 300,000 kW, 20 kV. These units were series produced.

Water cooling of the stator windings is accomplished by forcing water through internal channels in the conductors of the cores. The hollow conductors in the cores alternate with solid conductors. The ends of each rod are soldered to polepieces that have lugs for current connections and a chamber for the cooling water. The cooling water is fed to the chambers of these polepieces by insulation hoses from a ring-shaped header. Cooling of the rotor winding is by direct water feed of the TVF type.

In connection with the reduction in hydrogen consumption, a single-jet draft system was used for cooling the stator core with bilateral drawing of the gas from the gap between rotor and stator.

Turbogenerators of the TVV type are made on pedestal bearings. The bearing inserts are self-leveling with spherical support surface. Unitized housings are used in 150,000 and 200,000 kW machines with openings for the gas coolers, which are horizontally placed. A takedown housing is used in the 300,000 kW turbogenerators. In these units the length of the central part is approximately equal to the length of the active part, and the end sections of the housing, which are rectangular in shape, cover the end parts of the stator winding and accommodate the gas coolers and leads. The end parts are secured to the middle section. The 200,000 and 300,000 kW turbogenerators use an elastic suspension for the stator core. In the ribs of the stator on which the stator core is assembled, at the points where they are fastened to the walls of the housing, slots are cut through in the tangential direction so that the core is joined to the housing through a system of spring-like supports.

FOR OFFICIAL USE ONLY

The stator core is assembled of sheets of cold-rolled transformer steel with specific losses of the order of 1 W/kg.

The stator has a two-layer bar winding. The elementary conductors are transposed by 540° along the active part of the bar.

All fastening components of the end sections of the stator winding are made of nonmagnetic materials to reduce losses. A shield in the form of a copper ring is placed under the pressure plate. The teeth of the end stacks are made with slots.

The rotors are made of one-piece forgings. The rotor windings are made in the form of half-coils that are connected as they are placed in the rotor slots. Duralumin wedges are fastened in the grooved part of the winding, and nonmagnetic banding rings are fastened in the end sections.

The banding unit is doubled-seated in the TVV-200-2 and TVV-320-2 turbogenerators with seating on the rotor barrel with an elastic centering ring secured to the rotor.

The oil seal of the rotor shaft is an end seal with adjustable pressure of the seal insert.

In 1959 the Elektrot'yazhmash Plant made the first TGV-200 turbogenerator with power of 200,000 kW, and in 1961 produced the TGV-300 turbogenerator with power of 300,000 kW. These generators were based on the TVO-30 experimental turbogenerator.

The rotor winding is cooled in a bilateral axial arrangement of internal cooling of the conductors. The cooling gas is forced into the zone of the end sections, from which it flows through lateral input apertures into inner channels of the conductors through which it goes to the middle of the rotor and is thrown through a system of radial channels into the gap of the machine. The stator winding is cooled by a stream of gas flowing through metal tubes in bars situated between two vertical rows of elementary conductors. To ensure circulation of hydrogen in the machine, high-pressure squirrel-cage blowers are installed on one side of the rotor, and low-pressure fans are placed on the other side.

The stator core in TGV-200 turbogenerators is cooled in a radial arrangement, and in the TGV-300--in an axial arrangement.

The TGV-200 and TGV-300 turbogenerators are made on shield bearings. The bearings are installed in end shields with a horizontal split. The shields are secured to the stator housing.

The stator core is fastened in the stator housing on elastic hangers in the form of plate springs. The core is assembled in a comparatively light housing that is connected to the machine housing by steel plates.

A single-seated banding unit is used in the TGV-200 and TGV-300 turbogenerators with seating of the banding on the rotor barrel.

FOR OFFICIAL USE ONLY

The Novosibirsk Sibelektrotiyazhmash Plant began producing turbogenerators in the fifties. This plant mastered production of the TVF turbogenerators developed by the Elektrosila Plant with powers of 60,000 and 100,000 kW. In 1952 the plant made an experimental turbogenerator type TVM-60 with power of 60,000 kW of original design with oil-filled stator, water-cooled rotor winding, oil-paper insulation and internal oil-cooling of bars. TVM-300 turbogenerators with power of 300,000 kW [Ref. 8] were developed and put into production on the basis of the TVM-60.

The 200,000 and 300,000 kW turbogenerators were updated and improved during use. The most important changes involved using thermosetting insulation of the stator winding. At the same time, the systems for fastening the stator winding were improved, semiconducting wavy side liners were introduced in the grooved section, in the end sections, liners were used that were made of molding materials filling in the gaps between the bars and fastening components, self-seating Dacron cords were used.

Equalization of stiffness with respect to axes of symmetry was used in the rotors of the 300,000 kW turbogenerator.

The double-seated banding arrangement in turbogenerators of the TVV series was replaced by a single-seating arrangement with seating on the rotor barrel, the banding ring being fastened by a special sleeve nut. At the same time, a damper system in the form of a short-circuited lug was used on the rotor in TVV-320-2 turbogenerators.

Turbogenerators With Power of 500,000 kW. In 1954, the Elektrosila Plant made the first TVV-500-2 turbogenerator with power of 500,000 kW [Ref. 1].

The TVV-500-2, like other turbogenerators of this series, had direct water cooling of the stator windings, a single-jet draft arrangement for hydrogen cooling and direct hydrogen cooling of the rotor winding with gas takeoff from the gap.

Centrifugal blowers were used rather than axial fans, and the radial ventilation channels in the stator were 5 mm wide. The end sections of the rotor winding were cooled in a two-jet arrangement.

To reduce losses, the rotor winding had trapezoidal rather than rectangular slots, and the small coils of the winding were made with a reduced number of turns. To improve the thermal stability of the rotor in asymmetric regimes, a shorting ring was installed in the form of a two-layer copper lug overlapping the insulation covering the end sections of the rotor winding from the outside.

The banding ring of the rotor was seated only on the barrel and was prevented from axial displacements by a sleeve nut.

Subsequently during series production of turbogenerators, the system of fastening the stator winding in the end section was improved, and a tangential ventilation arrangement was introduced for the stator core.

In 1965, a TGV-500 turbogenerator with power of 500,000 kW and speed of 3000 rpm was made at the Elektrotiyazhmash Plant.

FOR OFFICIAL USE ONLY

In contrast to the lower-power turbogenerators of the Elektrot'yazhmash Plant, the TGV-500 had water-cooled rotor and stator windings.

Supply and return of the water to the stator winding was through special feed-through insulators. The connecting lines and end leads of the stator winding were also water-cooled. A special end seal was used for cooling water supply to the rotor. The water was fed through central orifices of the exciter and generator shafts to a distribution header, from which water lines brought it to the coils of the rotor winding which was connected in parallel with respect to water flow. The current feeder of the rotor was also water-cooled.

The generator used a single-jet radial core ventilation system with distribution from the gap. The pressure plates of the stator core were water-cooled.

Vibration isolation of the stator core was by leaf springs. As opposed to other turbogenerators of the TGV type, the springs were placed only in the vertical plane, and connected the sealed inner housing of the stator directly to the foundation. The end sections of the stator housing were covered by shields with elastic coupling to the core housing.

The generator bearings were accommodated in shields resting on the foundation.

Subsequently in putting the TGV-500 turbogenerators into series production, improvements were made in the system of fastening of the stator winding and core in the housing, and in the technique of soldering the rotor coils.

In 1978, based on experience in developing turbogenerators of the TVM series, the Sibelektrot'yazhmash Plant made the first TVM-500 turbogenerator with power of 500,000 kW for increased voltage of 36 and 75 kV. Like the TVM-300, this turbogenerator has an oil-cooled winding and core in the stator, and a water-cooled rotor winding. The stator winding has oil-paper insulation. The end stacks in the TVM-500 generator are beveled. The core is tensioned in the axial direction by bolts running through the back. Axial channels of rectangular shape are made in the core for cooling purposes. The stator winding bars are made up of solid conductors of short height. A cooling channel is formed between the conductor columns. The winding is held in the slots of the core by opposed wedges. The generator rotor has a hollow damping system formed by copper strips laid in the rotor slots and closed by copper lugs. The gap is cooled by the distillate circulating through tubes in shallow slots at the crowns of the teeth of the rotor barrel.

Turbogenerators With Power of 800,000 kW. In 1970 the Elektrosila Plant made the first turbogenerator with power of 800,000 kW type TVV-800-2 [Ref. 12].

In this turbogenerator there was a considerable improvement in the ventilation system, the design of the fastening for the stator winding and core, the damper system of the rotor, operation of the brush equipment, and the oil seals of the shaft.

A hydrogen gas tangential ventilation arrangement with counterrotation of the cooling hydrogen in the stator compartments was introduced for cooling the stator core. Internal channels were used in the rotor for the multi-jet system instead of the side channels in the 500,000 kW turbogenerator. Rotor cooling efficiency was

FOR OFFICIAL USE ONLY

considerably improved by installing axial barriers in the gap, and by improving cooling of the end sections of the rotor winding coils.

Opposed wedges and liners of molding materials were used to hold the stator windings in the slot. Monolithic fastening of the end sections of the winding was effected by using molding materials, epoxy cements, self-seating cords and massive fiberglass plastic rings. The design provided for continuous pressing of the end sections of the winding by wedges and titanium springs, and also by the capability for axial displacements of the winding with changing loads.

Core vibration was additionally reduced by increasing its elastic modulus, and by much better fastening of the core in the housing.

To reduce heating of the end stacks, the number of stepped end stacks of the core was increased, and cooling was improved.

Now in series production are 800,000 kW turbogenerators with hydrogen-water cooling. Seven of these generators are now being successfully used in power systems.

In addition to producing turbogenerators with water-hydrogen cooling, the Elektro-sila Plant is doing research on completely water-cooled turbogenerators [Ref. 7, 11]. This work was started in 1968 when the first experimental turbogenerator with power of 63,000 kW and speed of 3000 rpm was made. Successful operation of the experimental generator, and the results of studies on prototypes and models led to production of the first TZV-800 turbogenerator in 1978 with power of 800,000 kW and speed of 3000 rpm, totally water-cooled without hydrogen filling. The generator has direct water cooling of the windings of stator, rotor, and damping winding, stator core, structural components and brush apparatus. The volume of the machine is filled with nitrogen at low excess pressure.

A distinguishing feature of the system is the use of a self-pressurized arrangement for water-cooling of the rotor winding. Water runs freely into a ring header open to the shaft, is picked up by the turning rotor, goes to the lower leads of the coils, flows through the coils and leaves through the upper leads.

The stator core is cooled by flat silumin coolers containing coiled stainless steel tubing. The coolers take the form of active steel segments and are pressed between the stacks.

The core is elastically fastened only on the side walls of the stator.

The end sections of the stator winding are held between fiberglass plastic rings. Compression of the end sections is by springs and a system of tension members and thrust blocks. The end sections are held together by cold-setting epoxy cement.

The generator uses a complete damper winding placed beneath the slot wedges of the rotor. In the vicinity of the end sections, the bars of the damper winding are shorted by copper segments. The winding is also cooled by a self-pressurized arrangement.

The turbogenerator has been successfully tested on a stand in the Elektrosila Plant and has been put into experimental operation at a GRES.

FOR OFFICIAL USE ONLY

Turbogenerator With Power of 1.2 Million kW. In 1976 the Elektrosila Plant produced the largest two-pole turbogenerator in the world. Like the series-produced TVV-800-2 turbogenerator with power of 800,000 kW, the TVV-1200-2 (power of 1.2 million kW) has direct hydrogen cooling of the rotor winding in a multi-jet arrangement, the stator housing is filled with hydrogen, and the stator winding is made with direct water cooling. Cooling in the generator is intensified in the end sections of the core.

To ensure high reliability of the generator with increased use of the active volume, a six-phase configuration of the stator winding for the first time has replaced the traditional three-phase arrangement.

In connection with an increase in the excitation winding current (to 7720 A as compared with the 3800 A in the 800,000 kW turbogenerator), a brushless excitation system has been used. The exciter is made with two armatures and two magnet systems as part of a system for noncontact monitoring and measurement.

The turbogenerator has been successfully stand-tested at the plant, and has been put into operation.

Turbogenerator With Speed of 1500 rpm. In 1976, the Elektrotiyazhmash Plant finished making the first modern TGV-500-4 four-pole turbogenerator with power of 500,000 kW [Ref. 9]. The turbogenerator is designed around the features of the TGV-500 turbogenerator with 500,000 kW power and speed of 3000 rpm that is made by the same plant, and likewise uses direct water cooling of the windings of the stator and rotor and hydrogen filling of the stator housing.

The stator housing of the generator is made in three sections: the core with winding is assembled in the middle section, and the gas coolers and oil seals of the rotor shaft are accommodated in the end sections. The oil seals are of ring type with self-aligning inserts. Fastening of the stator windings is rigid with the use of molding materials, bracing wedges and cleats.

The generator rotor is composite. Banding rings of nonmagnetic steel are made with single seating. The end wedges of the rotor are of opposed type, made of bronze, fit tightly into the slot, and are driven into the slot with tight fit. The wedges overlap the joints in the region of the joints between rotor parts.

The generator uses a brushless exciter consisting of a synchronous inverted generator, rotating rectifier and inductor generator.

The turbogenerator combined with the brushless exciter has been stand-tested at the plant and is now in power plant operation.

In 1980 the Elektrosila Plant made and tested the first TVV-1000-4 turbogenerator with power of 1 million kW at a speed of 1500 rpm. The generator has the same cooling system and design as the series-produced TVV-800-2 with power of 800,000 kW. The rotor winding and stator core are hydrogen-cooled, and the stator winding is water-cooled.

The turbogenerator has increased current volume in the stator slot (up to 26 kA), and therefore particular emphasis has been placed on the fastening of the winding.

FOR OFFICIAL USE ONLY

The fastening of the winding in the slot was tested on a prototype. The design of the end stack of the core was improved. The number of core stacks was increased, and their cooling was improved. Improvements were also made in the cooling of the rotor windings, and subslot wedges were introduced in the zone of transition from the soltted section to the end section.

The rotor forging was of welded and forged construction.

Outlook for Future Development of Turbogenerator Construction. The next power stage will be turbogenerators with power of 1.6-2 million kW at 3000 and 1500 rpm. Analysis has shown [Ref. 2, 3, 4, 13] that generators of this power can be built on the basis of turbogenerators that have already been made and tested in the power range of 800,000-1,200,000 kW. It will be necessary to use rotor forgings of greater mass, and to do research on further improvement of cooling systems and the design of individual machine components.

A still further increase in power would have to be based on using the effect of superconductivity [Ref. 5], which is completely realistic, given the rapid progress in development of generators of this type.

REFERENCES

1. Borushko, V. S., Gnedin, L. P., Danilevich, Ya. B. et al., "500-MW Turbogenerators Produced by the Elektrosila and Elektrotyazhmash Plants", ELEKTROTEKHNIKA, No 1, 1970, pp 2-6.
2. Borushko, V. S., Glebov, I. A., Danilevich, Ya. B., et al., "Developmental Outlook and Ways to Improve Turbogenerator Design", Vsemirnyy elektrotekhnicheskiiy kongress [International Electrotechnical Commission], Moscow, 1977, IEC Report No 1.04, Moscow, 1977, 12 pp.
3. Glebov, I. A., Danilevich, Ya. B., "Nauchnyye problemy turbogeneratorostroyeniya" [Scientific Problems of Turbogenerator Construction], Leningrad, Nauks, 1974, 280 pp.
4. Glebov, I. A., Danilevich, Ya. B., "Current State and Problems of Developing Turbohydrogenerators and Synchronous Compensators", ELEKTRICHESTVO, No 3, 1976, pp 1-7.
5. Glebov, I. A., Danilevich, Ya. B., Shakhtarin, V. N., "Using Superconductivity in Electrical Engineering", ELEKTROTEKHNIKA, No 11, 1977, pp 17-18.
6. Glebov, I. A., Danilevich, Ya. B., Kurilovich, L. V. et al., "1000-MW 3000-rpm Turbogenerator", ELEKTROTEKHNIKA, No 3, 1978, pp 3-6.
7. Glebov, I. A., Danilevich, Ya. B., Iongansen, V. I. et al., "800-MW 3000-rpm Water-Cooled Turbogenerator", ELEKTRICHESTVO, No 2, 1980, pp 3-8.
8. Gnedin, L. P., Danilevich, Ya. B., Maslennikov, K. N., "TVM-300 Turbogenerator With Water-Oil Cooling", ELEKTROTEKHNIKA, No 1, 1970, pp 6-8.
9. Grinchenko, N. G., Danilevich, Ya. B., Kil'dishev, V. S., Levitskiy, A. K., "TGV-500-4 Turbogenerator", ELEKTROTEKHNIKA, No 7, 1977, pp 22-23.

FOR OFFICIAL USE ONLY

FOR OFFICIAL USE ONLY

10. Kostenko, M. P., Borushko, V. S., Danilevich, Ya. B. et al., "Turbogeneratory: Nauchno-tekhnicheskiy obzor. Elektrotekhnicheskay promyshlennost' SSSR" [Turbogenerators: Scientific-Engineering Overview. Electrical Engineering Industry of the USSR], Moscow Informstandartelektro, 1967, 599 pp.
11. Shapiro, A. B., Chernyavskiy, V. P., Kari-ogly, I. A., Danilevich, Ya. B., "Totally Water-Cooled Experimental Turbogenerator", ELEKTROTEKHNIKA, No 2, 1974, pp 1-4.
12. Chistikov, A. P., Glebov, I. A., Danilevich, Ya. B., Khutoretskiy, G. M., Mamikonyants, L. G., Romanov, V. V., "The 800 and 1200 MW Two-Pole Turbogenerators. Design Features and Test Results", CIGRE Report No 11-03, 1978, 6 pp.
13. Glebov, I. A., Danilevich, Ya. B., "Grenzleistungen von Turbogeneratoren und Entwicklungsperspektiven des Turbogeneratorenbaus in der UdSSR", ELEKTRIE, Vol 33, No 1, 1979, pp 10-13.

COPYRIGHT: IZDATEL'STVO "NAUKOVA DUMKA", "TEKHNICHESKAYA ELEKTRODINAMIKA", 1980

6610

CSO: 1861/24

FOR OFFICIAL USE ONLY

FOR OFFICIAL USE ONLY

UDC 621.311.083.72

REMOTE MEASUREMENT OF ELECTRICAL ENERGY AND AVERAGE POWER IN POWER SYSTEMS

Moscow ELEKTRICHESTVO in Russian No 6, Jun 81 (manuscript received 15 Mar 79) pp 2-6

[Article by V.A. Bogdanov, Central Dispatching Administration for the USSR Unified Power System Integrated Power Grid]

[Text] The control, planning and analysis of power systems operating modes are realized on the basis of information, an important component of which is measurements of electrical power and energy. The automated control and operational monitoring are based on remote measurements (TI) of the power, where these measurements are transmitted via multichannel pulse code remote control units (UTM), with reset cycles which have a length of $T_i < 20$ sec. The planning and analysis of operating modes are predicated on hourly measurements of the power, transmitted via data transmission equipment, teletype and telephone as part of the daily dispatcher control sheet.

At the present time, extremely important parameters for dispatcher control are lacking in the remote measurements and the daily control sheet: the electrical power generated by the main electric power stations, power overcurrents on inter-system and interstate power transmission lines, electrical power consumption in the major load centers, etc. The values of the indicated parameters are needed by the dispatcher for various time intervals: an hour, a work shift, the peak load period, etc.

Remote measurements are especially needed for the increments of electrical power for the monitoring and control of power overcurrents in the "USSR -- CEMA Member Nations" section, where half-hourly metering periods are employed. The derivation of the indicated parameters by the interpolation of measurements of the instantaneous power values yields an impermissibly large error.

The organization of remote measurements of power increments and the average power by means of electronic power metering counters which have multichannel pulse-code remote control units, communications channels and ASDU [automated dispatcher control system for a power association] computer hardware is treated in this article.

The electronic counters (ES) are produced by the Vil'nyus Plant for Electrical Measurement Equipment (F-441) and the Leningrad Electromechanical Plant (F-651). Electronic counters are produced abroad by a whole series of companies. For

FOR OFFICIAL USE ONLY

FOR OFFICIAL USE ONLY

example, the Swiss company of Landis and Gyr (Tettex AG Instruments) produces a large assortment of electronic counters which are used in the power systems of CEMA member nations. An extremely important advantage of electronic counters over conventional electromechanical meters is the high level of precision (0.1--0.5). For this reason, it is planned that active and reactive power will be metered by means of electronic counters in the immediate future at all of the largest electric power stations and on intersystem and interstate links.

An electronic counter is an analog-digital device in which one can single out the following main components: the measurement unit, IO; the divider circuitry, DS; the crystal oscillator, GK; the readout display, BI; and the counting mechanism, SM.

The currents I_i and voltages U_i from the instrument transformers for each phase are fed to the input of the measurement unit. Using the principle of double modulation, the measurement units converts I_i and U_i to a numerical pulse code. The number of pulses N at the output of the measurement is proportional to the quantity of electrical power in the forward (f) and return (r) direction over the measurement period T_0 :

$$N_f = \sqrt{3} I_{i1}^f U_{i1} T_0 C_{0e}^{-1}; \quad N_r = \sqrt{3} I_{i1}^r U_{i1} T_0 C_{0e}^{-1} =$$

$$N_n = \sqrt{3} I_n^a U_n T_0 C_{0e}^{-1}; \quad N_o = \sqrt{3} I_n^o U_n T_0 C_{0e}^{-1}, \quad (1)$$

where C_{0e} is the pulse value equal to the quantity of electrical power associated with each pulse at the output of the measurement units.

If the measurement unit segregates the active component, $I_{i.act.}$, the electronic counter measures the active power. In the case where $I_{i.react.}$ is used in (1), the reactive power is metered. Thus, for example, the type F-441 electronic counter provides for simultaneous metering of the active and reactive forward and return power.

The DS divider circuitry consists of electronic circuits which reduce the frequency of the signals incoming from the measurement unit and the crystal oscillator. Pulsed signals can be obtained from the outputs of the divider circuitry, the frequency of which is the requisite number of times less than the frequency at the input. The forward and return power metering signals, which are fed to the input of the counting mechanism, have a frequency which is β_1 times less than the frequency of the N_f and N_r signals at the input to the divider circuitry. The coefficient β_1 is chosen by working from the capacity of the counting mechanism, the precision class of the instrument and the requisite periodicity and duration of continuous electrical power metering (without zeroing the counting mechanism).

The readout display is intended for visually monitoring the operation of the electronic counter. For this reason, the signals fed to the display input have a

FOR OFFICIAL USE ONLY

FOR OFFICIAL USE ONLY

frequency which is β_0 times less than the frequency of the N_f and N_r signals. The value of β_0 is chosen so that at the minimum value of I_1 , no less than one pulse every 10 to 15 seconds is fed to the input of the readout display.

The crystal oscillator is the source of the f_0 frequency which controls the operation of the divider circuitry, as well as the measurement unit modulator and converter. To compensate for the zero drift in the counter characteristics, a periodic change is made in the polarity of the modulator output signal by means of the crystal oscillator signals and the output pulses of the measurement unit converters are switched accordingly. The divider circuitry produces the requisite signals at a frequency α_1 times less than f_0 .

Thus, electric power metering signals can be obtained from an electronic counter with a pulse value of $\beta_1^{-1} C_{0e}$, as well as crystal oscillator signals at a frequency of $\alpha_1 f_0$. This makes it possible to use electronic counters for remote transmission of power values $E(T_0)$ and average values of the power over the measurement period $W(T_0)$ by means of existing multichannel pulse-code remote control units. Moreover, electronic counters can be used for the measurement of $E(T_0)$ and $W(T_0)$ directly in a power facility. In this case, the electronic counter is used as a meter, from the output of which the numerical code for the parameter being measured is fed to the digital or analog readout of the corresponding instrument.

In the latter case, the numerical code of the parameter being measured should be preconverted to an analog signal by means of digital to analog converters. For the direct measurement and remote measurement of $E(T_0)$ and $W(T_0)$, the existing electronic counters must be complemented with special interfaces.

An interface* incorporates the following: a bidirectional counter RS, which contains nine bits; an SB circuit which blocks the arrival of power metering pulses at the inputs to the bidirectional counter; an SU circuit which sets the bidirectional counter to the initial state; a parallel carry circuit SPP, an eight bit output register VR and a switch P.

The position of the switch determines the value of the power metering pulses and the crystal oscillator signal frequency incoming from the divider circuit. For any setting of the switch, pulses are fed from it which set all flip-flops of the divider circuitry registers to zero, where these flip-flops reduce the frequency of the crystal oscillator and feed out the $\alpha_1 f_0$ signals. It is expedient to transmit $E(T_0)$ over periods of one hour or less, but necessarily submultiples of one hour. For this reason, to synchronize the start of power readout for various facilities with astronomical time, any change in the position of the switch should be made by servicing personnel after each repair and check of the electronic counter and the interface at the start of any time interval based on precision time signals.

* Staff members of the Central Dispatcher Administration for the Integrated Power Grid of the USSR Unified Power System participated in the design of the interface: V.M. Chizhkov, S.S. Raksheyev and U.K. Kurbanganliyev.

FOR OFFICIAL USE ONLY

FOR OFFICIAL USE ONLY

The $\beta_1 N_f$ pulses are fed to the adding input, while $\beta_1 N_r$ are fed to the subtract input of the bidirectional counter through the SB blocking circuit.

The SB blocking unit, in accordance with the $\alpha_1 f_0$ signal incoming from the divider circuit, blocks the arrival of the electrical power metering pulses at the inputs of the bidirectional counter. Right after this, the parallel carry circuit carries the contents of the bidirectional counter to the output register. The carry is accomplished taking into account the state of the lowest order ninth digit of the bidirectional counter, the contents of which are added before this to the contents of the eight high order digits of the bidirectional counter. After completing this procedure, the SU reset circuit sets the bidirectional counter to the initial state, while the SB blocking circuit enables the pulses to get to the bidirectional counter.

If the measurement is made in a section with bidirectional power flows, the amount of electrical power is:

$$E(T_0) = K_I K_U \beta_1^{-1} C_{0e} (N_c - N_y) = \mathcal{P}(T_0) = K_I K_U \beta_1^{-1} C_{0e} (N_c - N_y),$$

where K_I and K_U are the transformation ratios of the current and voltage instrument transformers; $N_c = (N_f - N_r) \beta_1 + N_y$ is the number of pulses registered by the bidirectional counter at the measurement period; N_y is the number of pulses in the initial state of the bidirectional counter, specified by the SU reset circuitry.

If the power is transmitted only in the forward direction, $N_y = 0$. When measuring the power transmitted only in the return direction, $N_y = 512$.

Thus, the measurement period is governed by the frequency incoming from the divider circuitry to the inputs of the SB blocking circuitry, the SU reset circuit and the parallel carry circuit: $T_0 = (\alpha_1 f_0)^{-1}$, and is numerically equal to the time between two successive data updates at the output register.

The remote transmission of $E(T_0)$ using the multichannel pulse-code remote control units in service at the present time can be accomplished in the form of telemetry signals in a "remote measurement repeating" mode. In both cases, the parameters of the output register should be matched to the parameters of the remote control unit with respect to the input impedance.

In the case of the cyclical transmission of $E(T_0)$, the following condition should be met to avoid data losses and distortion:

$$\begin{aligned} t_{st} &\leq 0.5V^{-1}; & t_{b,n} &\leq 0.5V^{-1}; \\ t_{cyc} &\leq T_0 & T_n &\leq T_0, \end{aligned}$$

FOR OFFICIAL USE ONLY

where t_{st} is the switching time of the output register elements of the interface; V is the telemetry data transmission rate through the communications channel; T_{cyc} is the duration of the renewal cycle with which the transmission of the telemetry data is accomplished.

If $E(T_0)$ is transmitted sporadically, then the following condition must be met to avoid data losses and distortions:

$$T_0 \geq T_m,$$

where T_m is the maximum time from the moment of query appearance (a change in the state of the output register digits) until the completion of the transmission of the group of telemetry signals, in which $E(T_0)$ is transmitted.

Power measurement precision can be characterized by the referenced total mean square error [1]. When using transducers with a standard analog output signal, the mean square reference error for remote power measurements is:

$$\bar{\delta}_r = \sqrt{\bar{\delta}_I^2 + \bar{\delta}_U^2 + \bar{\delta}_n^2 + \bar{\delta}_{n.n}^2 + \bar{\delta}_{o.n}^2 + \bar{\delta}_k^2 + \bar{\delta}_a^2 + \bar{\delta}_{mp}^2}. \quad (2)$$

The components of the overall referenced mean square error indicated in (2) are due to the following: $\bar{\delta}_I$ and $\bar{\delta}_U$ of the current and voltage instrument transformers; $\bar{\delta}_n$ from the transducer which converts the parameter being measured to a standard analog signal; $\bar{\delta}_{p.n}$ and $\bar{\delta}_{o.n}$ from the level quantization of the sensor signal during transmission and the back-conversion of the digital code to analog form at the receive end (the static error); $\bar{\delta}_k$ from the communications channel; $\bar{\delta}_d$ from the time quantization of the sensor signal (the dynamic error); $\bar{\delta}_{mp}$ from the analog meter.

When the measurements are fed into a digital computer, there is no need for converting the received code to analog form or the corresponding meter. In this case, one can use $\bar{\delta}_{o.n} = \bar{\delta}_{mp} = 0$.

The codes employed in modern remote control units provide for a sufficiently high level of protection of the transmitted data against interference in the channel and make it possible to not only detect, but in a number of cases correct distortions which appear. For this reason, it can be assumed that in those cases where the remote measurements, following transmission through the communications channels, are not rejected by the interference protection system, $\bar{\delta}_k = 0$ [2].

The overall mean square referenced error of a measurement on a unit is:

$$\begin{aligned} \bar{\delta}_r^2 &= \sqrt{\bar{\delta}_I^2 + \bar{\delta}_U^2 + \bar{\delta}_{mp}^2 + \bar{\delta}_c^2}; \quad \bar{\delta}_r^4 = \\ &= \sqrt{\bar{\delta}_I^2 + \bar{\delta}_U^2 + \bar{\delta}_{mp}^2 + \bar{\delta}_{a.n}^2} \end{aligned}$$

FOR OFFICIAL USE ONLY

FOR OFFICIAL USE ONLY

where $\bar{\delta}_\Sigma^a$ corresponds to the analog measurement, while $\bar{\delta}_\Sigma^u$ to the digital measurement; $\bar{\delta}_c$ is the mean square referenced error in reading the analog meter readings; $\delta_{д.п.}$ is the dynamic error which is due to the discrete nature of the renewal of the readings of the digital meter.

For analog measurements, $\bar{\delta}_c$ fluctuates in a wide range and is independent of the form, dimensions or linearity of the instrument scale, as well as the distance and angle of observation, periodicity and time of readout, skill level of the personnel, etc. When using digital instruments, $\bar{\delta}_c = 0$.

If the measurements on site and the remote measurements are made from common instrument transformers and the precision class of the analog meters used on site and those for reproducing the remote measurements match, then the measurement error is equal in all levels of the dispatcher hierarchy if:

$$\bar{\delta}_n^2 + \bar{\delta}_{n.n}^2 + \bar{\delta}_{o.n}^2 + \bar{\delta}_a^2 = \bar{\delta}_c^2.$$

When digital meters are used on the unit and the remote measurements are fed to the digital computer with a subsequent digital display, equal precision of the measurements at all levels of the dispatcher hierarchy is assured if:

$$\bar{\delta}_n^2 + \bar{\delta}_{n.n}^2 + \bar{\delta}_a^2 = \bar{\delta}_{np}^2 + \bar{\delta}_{a.n}^2.$$

The dynamic error of a remote power measurement is [2]:

$$\begin{aligned} \bar{\delta}_a^2 &= 2D_x \Delta_x^{-2} \left[1 - T_u^{-1} \int_n^{T_n+T_u} K_s(\tau) d\tau \right] = \\ &= D_x \Delta_x^{-2} (T_u + 2T_n) T_n^{-1}, \end{aligned} \quad (3)$$

where D_x and T_k are the dispersion and the time constant for the normalized autocorrelation function of the parameter being measured; Δ_x is the measurement range; $T_\pi = T_u r^{-1}$ is the time for transmitting one remote measurement via the communications channel, when r parameters are transmitted during each update cycle of length T_u .

The overall referenced mean square error in a measurement of $E(T_0)$ transmitted to the output register of the interface is:

$$\bar{\delta}_{\Sigma} = \sqrt{\bar{\delta}_I^2 + \bar{\delta}_U^2 + \bar{\delta}_{\Sigma,c}^2 + \bar{\delta}_0^2},$$

where $\bar{\delta}_{\Sigma,c}$ is the mean square referenced error of the measurement unit of the electronic counter, which is determined by the precision class of the instrument; $\bar{\delta}_0$ is the component of $\bar{\delta}_{\Sigma}$ which is due to the digital manner of obtaining $E(T_0)$.

In the case of a fixed number of output register bits, $\bar{\delta}_0$ depends on the length of T_0 , the chosen value of the pulses $C_{\beta e} = \beta_1^{-1} C_{0e}$ and the time interval t_{b1} , during

FOR OFFICIAL USE ONLY

FOR OFFICIAL USE ONLY

which the SB blocking unit blocks the feed of the power metering pulses to the inputs of the directional counter. If the values of $E(T_0)$ within the time interval between two successive power metering pulses are distributed uniformly, then:

$$\delta_0 = \sqrt{\{C_{\beta\beta} [3(I_{H.M.}^n + I_{H.M.}^o) U_H^2 T_0^{-1}]^2 + \frac{1}{3} [t_{\text{con}} T_0^{-1}]^2\}} \quad (4)$$

where $I_{H.M.}^n$ and $I_{H.M.}^o$ are the maximum possible absolute current values for the instrument circuit, which correspond to the forward and return electrical power transmission directions; U_H is the nominal instrument circuit voltage.

To avoid bidirectional counter overflow during the measurement period, the value of a power metering pulse should be chosen from the condition:

$$\sqrt{3} (I_{H.M.}^n + I_{H.M.}^o) U_H^2 T_0 < 512 C_{\beta\beta}.$$

The number of pulses in the initial state of the bidirectional counter, specified by the SU reset circuit:

$$N_y = C_{\beta\beta}^{-1} \sqrt{3} I_{H.M.}^o U_H^2 T_0.$$

The average value of the power over the measurement period T_0 is:

$$W(T_0) = K_I K_U (N_c - N_y) C_{\beta\beta} T_0^{-1} = K_I K_U (N_c - N_y) C_{\beta w},$$

where $C_{\beta w} = C_{\beta\beta} T_0^{-1} = [C_{\beta\beta} T_0^{-1}]$ is the value of a pulse in the conversion of the output register readings to power units.

Since the master crystal oscillator of the counter provides for high stability in T_0 , the error in determining $W(T_0)$ is practically equal to the measurement error for the energy increment transmitted to the output register.

When measuring $W(T_0)$, the actual power graph will be represented at the receive end by a step function, the ordinate of each step of which is numerically equal to the average power over the preceding ongoing measurement period. For this reason, the referenced dynamic mean square error of the measurements of the average power values is to be understood as:

$$\begin{aligned} \delta_{\text{acc}}^2 &= \Delta_x^{-2} M(X_n - X_T)^2 = \Delta_x^{-2} M[\bar{X}_{i-1} - X_i]^2 = \\ &= \Delta_x^{-2} M[\bar{X}_{i-1}^2 - 2\bar{X}_{i-1} X_i + X_i^2], \end{aligned} \quad (5)$$

where M is the universal mean value; X_H and X_T are the measured and precise values of the parameter; $\bar{X}_{i-1} = M(X_{i-1}) = T_0^{-1} \int_{t_{i-1}}^{t_i} W(t) dt$ is the average value of

FOR OFFICIAL USE ONLY

the power in the preceding measurement period; $X_i = W(t) \Big|_{t_i}^{t_i+T_k}$ is the current value of the power in the i -th (current) period.

Taking the adopted symbols into account, $M(X_i)^2 = D_X$ is the dispersion of the random quantity X_i .

In steady-state modes, the autocorrelation functions of the power [3] are:

$$K_x(\tau) = D_x e^{-\tau/T_k}.$$

In accordance with this, the spectral density of the parameters being measured is [2]:

$$S(\omega) = D_x T_k [\pi(1 + T_k^2 \omega^2)]^{-1}.$$

The following mutual relationships exist between the dispersion, the autocorrelation function and the spectral density:

$$D_x = K_x(0) = 2 \int_0^\infty S(\omega) d\omega; \quad (6)$$

$$K_x(\tau) = 2 \int_0^\infty S(\omega) \cos \omega \tau d\omega. \quad (7)$$

If it is assumed that the integral portion of the measurement unit of the electronic counter has the characteristics of an ideal filter, then there will be no frequencies in the spectrum of the random quantity \bar{X}_{i-1} which have a period less than T_0 . Then, when determining the numerical characteristics for \bar{X}_{i-1} , the upper limits of the integrals (6) and (7) will be equal to $\omega_{\max} = 2\pi T_0^{-1}$.

Taking what has been presented above into account, the dispersion of the random quantity \bar{X}_{i-1} is:

$$\begin{aligned} M(X_{i-1})^2 = D_{\bar{X}} &= 2D_x T_k \pi^{-1} \int_0^{2\pi T_0^{-1}} (1 + T_k^2 \omega^2)^{-1} d\omega = \\ &= 2D_x \pi^{-1} \operatorname{arctg} 2\pi T_k T_0^{-1}. \end{aligned} \quad (8)$$

Since it is expedient to measure $W(T_0)$ over periods of $T_0 \ll T_k$, while the integral portion of the electronic counter is not an ideal high pass filter, it follows from (8) that $D_{\bar{X}} \approx D_X$, i.e., the dispersions of \bar{X}_{i-1} and X_i are numerically equal to each other.

It can be proved in a similar manner from (7) that when $T_0 \ll T_k$, the autocorrelation functions of X_i and \bar{X}_{i-1} coincide. In this case:

$$M(\bar{X}_{i-1}, X_i) \approx K_x(\tau) = D_x e^{-\tau/T_k}. \quad (9)$$

FOR OFFICIAL USE ONLY

Substituting (9) in (5), taking into account the delay during transmission and readout of the measurements in the digital computer memory, we obtain:

$$\delta_{\Delta}^2 = 2D_x \Delta_x^{-2} \left[1 - T_0^{-1} \int_{t_n}^{t_n + T_0} e^{-\tau/T_0} d\tau \right].$$

Consequently, the total referenced mean square error of remote measurements of the instantaneous values of the power and $W(T_0)$ are the same if they are made from common instrument transformers, where the sensors and the electronic counters are of the same class of precision and the reset cycles and averaging period are equal.

The practical realization of measurements of $E(T_0)$ and $W(T_0)$ is primarily expedient on the units where the electronic counters are installed for purposes of metering and there are remote control units with back-up subchannels. Measurements of $W(T_0)$ can be treated as the equivalent of remote measurements of instantaneous power values. For this reason, it is expedient to transmit them with periods close to the renewal cycle, with which the remote measurements of the parameters needed for automated control and monitoring are transmitted.

It is expedient to transmit $E(T_0)$ with periods of $T_0 = l^{-1}$ hours, where l is any integer. If it is necessary to transmit $W(T_0)$ and $E(T_0)$ from the same unit, two identical interfaces are connected to the electronic counter. A value of T_0 , close to T_{cyc} , with which the remote measurements of the other parameters are transmitted, is set on one unit by means of the switch P . Then, based on precise time signals, the position of the switch P is set on the second unit which provides the requisite periodicity for the measurement of the energy increments.

When using remote control units which provide only for the cyclical transmission of the remote measurements and telemetry signals, one subchannel each is set aside for the transmission of $W(T_0)$ and $E(T_0)$. The energy increment is transmitted as many times as the specified time interval is greater than the reset cycle of the remote control unit. In the sporadic case, $W(T_0)$ and $E(T_0)$ are transmitted until the arrival of signals via a feedback channel which confirm the correctness of the reception. In both cases, losses of $E(T_0)$ are possible because of failures of the remote control unit and the communications channels only in the case of failures which last longer than the measurement period.

BIBLIOGRAPHY

1. Lozitskiy B.N., Mel'nichenko I.I., "Elektroradioizmereniya" ["Electrical Radio Measurements"], Moscow, Energiya Publishers, 1976, 224 pp.

FOR OFFICIAL USE ONLY

FOR OFFICIAL USE ONLY

2. Malov V.S., Dmitriyev V.F., "Kodoimpul'snyye teleizmeritel'nyye sistemy" ["Pulse Code Telemetry Systems"], Moscow, Energiya Publishers, 1969, 192 pp.
3. Bogdanov V.A., Sovalov S.A., Chernya G.A., "Teleinformatsiya v avtomatizirovannykh sistemakh dispetcherskogo upravleniya" ["Remote Telemetry Data in Automated Dispatcher Control Systems"], ELEKTRICHESTVO [ELECTRICITY], 1974, pp 1-6.

COPYRIGHT: Energoizdat, "Elektrichestvo", 1981

8225

CSO: 8144/059

FOR OFFICIAL USE ONLY

FOR OFFICIAL USE ONLY

CURRENT STATE AND PROBLEMS OF TRANSFORMER CONSTRUCTION DEVELOPMENT

Kiev TEKHNIЧЕСКАЯ ЭЛЕКТРОДИНАМИКА in Russian No 6, Nov-Dec 80 (manuscript received 21 Aug 80) pp 38-45

[Article by I. D. Voyevodin, director of the All-Union Institute of Transformer Construction, and O. I. Sisunenko, deputy director of the All-Union Institute of Transformer Construction, Zaporozh'ye]

[Text] The resolutions of the Twenty-Fifth Congress of the CPSU emphasize the importance of ongoing development of the power industry in the USSR.

One of the sectors of the national economy of the nation that ensures development of the electric power industry is transformer construction.

Progress in transformer construction is based on perfecting designs, considerably improving the properties of the magnetic and insulating materials that are used, perfecting production technology and developing present-day production capabilities.

Fig. 1 shows the growth in power of three-phase transformers and groups consisting of single-phase units.

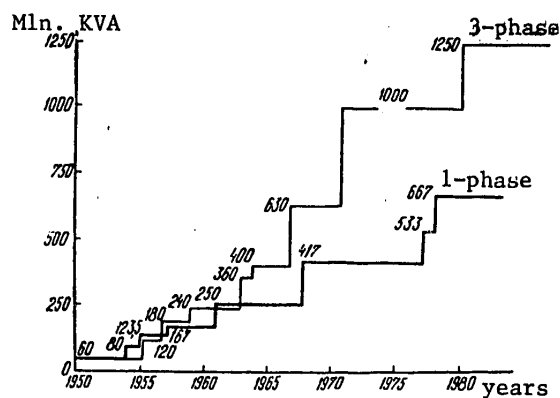


Fig. 1

FOR OFFICIAL USE ONLY

At present in the Soviet Union transformers with high voltage up to 330 kV inclusive are being made only in the three-phase version, for voltage of 500 kV--in single-phase and three-phase modifications, and for 750 kV and up--only single-phase. In the Tenth Five-Year Plan, industry has mastered production of a 1000-MVA transformer for voltage of 330 kV. In 1978 the first autotransformer with power of 667 MVA (2000 MVA in a three-phase group) and winding voltage combination of 1150/500 kV was made and delivered for experimental operation in a special power-grid stand.

The development of high-power transformers is tied up with a rise in generator power, since the most economic solution for electric power plants is the development of generator-transformer units. But since the energy produced by the electric power plants has to be transformed to different voltages, there has been a sharp rise in the research and development of transformers. Table 1 shows the powers of transformers for energy-producing units of different voltages.

TABLE 1

Power of unit, MW	Transformer power (MVA) at voltage (kV)					
	110	150	220	330	500	750
300	400	400	400	400	400	—
500	—	—	630	630	630	—
800	—	—	1000	1000	1000	—
1000	—	—	—	1250*	—	3×417
1200	—	—	—	—	3×533	—

* In the stage of assimilation.

To provide coupling and interflow of energy between systems with different voltages, a number of autotransformers of different power must be made with different voltage combinations.

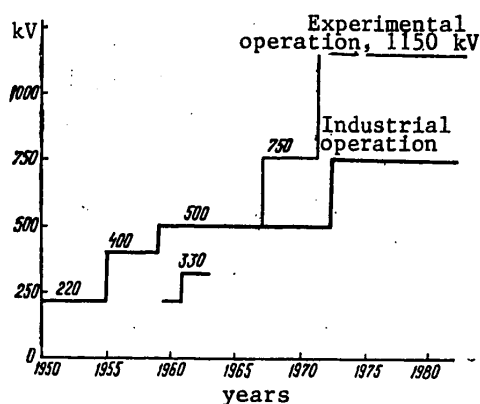


Fig. 2

FOR OFFICIAL USE ONLY

FOR OFFICIAL USE ONLY

Fig. 2 shows the increase in nominal voltage of transformers in the postwar period. The sixties saw a period of intense development of 330 and 500 kV power grids. Electric transmission lines of 750 kV were built in the seventies. Autotransformers with power of 333 MVA and voltage combination of 750/330 kV, and with power of 417 MVA and voltage combination of 750/500 kV were developed and produced for these lines. Industrial delivery of autotransformers for electric transmission lines of 1150 kV is planned for the beginning of the Eleventh Five-Year Plan.

In the seventies, industry mastered production of transformers and a reactor for power transmission lines on a voltage of ± 750 kV. These are in experimental operation on a test stand in the city of Tol'yatti. These transformers are essentially ready for use in ± 750 kVDC power transmission lines. However, to improve transmission economy, work is now in progress on higher-power transformers (320 MVA instead of 175 MVA).

The production of transformer equipment for 500, 750 and 1150 kV has covered the prospects for development of the electric power industry. On the other hand, solution of the problem of material inputs in transformer construction depends primarily on the technical level of transformers in classes of 6-10, 35 and 110 kV. The demand for materials in these classes makes up more than 80% of the total requirements of transformer construction. Therefore in recent years considerable attention has been devoted to development of 110-kV transformers. Industry has mastered production of the first types of three-phase 110-kV transformers with load-switching regulator in which wood laminate plastics are used, as well as lead-ins with solid insulation, and also reinforced wire. This has reduced the inputs of ferrous metals by 35% and cut open-circuit losses by 28%. Full-scale introduction of this series will in future keep the parameters of 110-kV transformers at the level attained by the leading non-Soviet companies.

The Eleventh Five-Year Plan calls for introducing a new series of 35-kV transformers with power of 1000-6300 kVA. Material inputs for transformers of this series have been reduced by a factor of 1.5. The savings in rolled ferrous metal stock will amount to 500 metric tons per million kVA of output.

A new series of transformers for voltage of 10 kV at power of 25-630 kVA has now been designed and is being put into production with technical characteristics on a level with analogs of leading non-Soviet companies. A distinguishing feature of the design of these transformers is the coiled spatial structure of the magnetic circuit. On the first stage, introduction of the new series is being done on the basis of traditional aluminum wires with paper insulation and radiator tanks. Any further increase in the technical level of this series presupposes the use of aluminum enameled wires and corrugated tanks.

Development of present-day transformers is based on advancing development of research on the various aspects of transformer construction.

To develop transformers with prospective voltages, a number of steps are being carried out to severely limit lightning and commutation surges, including the development of new arresters.

Based on generalization of studies on permissible field intensities in oil-barrier insulation, permissible field strengths have been established in the channels adjacent to the windings, and requirements have been worked out for the design,

FOR OFFICIAL USE ONLY

FOR OFFICIAL USE ONLY

technological processes and testing of an experimental transformer. The experimental ORTs-135000/500 transformer is intended for replacement of OTsG-135000/500 transformers at the Volzhskaya GES to verify the method of selecting the internal insulation with respect to prolonged action of the working voltage under operating conditions.

A considerable reduction in test voltages of the 500 kV winding as compared with State Standard GOST 1516.1-76 (by 30-40%) has enabled a reduction by more than 30% in the dimensions of the main insulation between windings and to grounded sections, as well as reducing the dimensions of longitudinal insulation (see Table 2).

TABLE 2

Characteristic	Unit of measurement	OTsG-135000/500 1960	ORTs-135000/500 1978 (plan)	ORTs-135000/500 (experimental)
Nominal power	MVA	135	135	135
Nominal voltage	kV	525/3	525/3	525/3
Test voltage of the high-voltage winding:				
total lightning stroke	kV	1500	1550	900
clipped lightning stroke	kV	180	1650	1000
commutation pulse	kV	--	1300	850
Short-circuit voltage	%	12.9	13	13.3
Open-circuit losses	kW	448	160	110
Short-circuit losses	kW	425	450	385
Mass of copper	tons	15.7	18.3	17.7
Mass of transformer steel	tons	108.4	91.3	66.7
Mass of transformer oil	tons	86	40	23
Total mass	tons	296	200	145
Transport mass	tons	--	140	127
			without oil	with oil

The encouraging results of work with the ORTs-135000/500 transformer opens up the possibility of considerably reducing material inputs of transformers for high voltage classes.

Construction quality is determined to a great extent by the availability of reliable design methods. Development of new methods of calculation and improvement of existing ones is one of the important areas of research and development over the last decade. Techniques have been developed for calculating magnetic and electric fields, additional losses in structural components, lightning and commutation surges in complex windings, current distribution in multiparallel windings. Development is nearing completion on an improved method of calculating the electrodynamic strength of transformer windings, a new technique has been developed for mechanical calculation of complicated components like the tank and pressing beams. Methods are being developed for optimization calculations in selection of variants. Extensive computerization of engineering calculations has considerably facilitated the

FOR OFFICIAL USE ONLY

FOR OFFICIAL USE ONLY

work of the designer, provided more in-depth computational analysis of items being designed, and improved the reliability of design features. The same can be said of the wide use of methods of physical and mathematical modeling in feasibility studies and also in research and development.

At present, work is near completion on development of a computational subsystem, and by the end of the Eleventh Five-Year Plan the graphic subsystem of the system for automated design of transformers is to be put into operation.

Improvements are continuously being made in design of the major components of transformers, which is conducive to the constant improvement of the technical characteristics, reduction of material inputs and increased operational reliability.

The magnetic circuits of power transformers are of grain-oriented rolled transformer steel 0.3-0.35 mm thick with losses of $P_{1.5} = 0.95-1.02$ W/kg. The use of fiberglass plastic banding has eliminated the holes in the steel for rods, reducing the level of losses and the open-circuit current. Currently work is being done in cooperation with metallurgists to develop transformer steel with low residual stresses, which in the future will eliminate process annealing of steel at transformer plants.

Open-circuit losses can be further reduced by making a magnetic circuit with complete diagonal joining, further improving the quality of transformer steel (reducing the specific losses to $P_{15} = 0.8-0.82$ W/kg).

In transformers with power of 25-630 kVA the open-circuit characteristics are considerably improved by introducing a three-dimensional design of magnetic circuits made of coiled elements.

At the present time in power transformers the windings for voltages up to 35 kV are helical with a large number of parallel conductors, the 110-330 kV windings are continuous coils, for 500 kV or more the windings are looped. Special steps to reduce intercoil gradients with pulse factors in continuous windings have obviated the need for shields and additional coil insulation. In looped windings, arrangements have been developed that give good distribution of voltages between individual sections and segments of the windings with resultant high pulse strength of the entire insulation structure. Transposed wires have been extensively introduced, reducing additional losses in the windings and improving labor productivity in making them.

Further research should be aimed at finding a lightning-proof design for transformer windings at the power limit, i. e. windings that have good distribution of pulse voltages and can pass a current of 3 kA.

The improvement of high-voltage transformer insulation involves further studies of oil-barrier designs, the use of rigid specially shaped insulating components for inhomogeneous field sections. A considerable part is played in this question by development of improved equipment and techniques for making such components, cleanliness and dust-free conditions in production departments, technology for drying insulation. Research aimed at improving the main insulation of transformers is an ongoing process involving the entire arsenal of scientific and technical capabilities, computer calculations, mathematical modeling on semiconducting paper

FOR OFFICIAL USE ONLY

and in an electrolyte bath, testing prototypes of components and complex models of insulation in full scale. Multifaceted studies result in reliable design solutions in the area of electric insulation for transformers.

A primary part in development of transformers at the limit of power is played by expert designing of components from the standpoint of eddy losses caused by leakage fluxes of the windings. Any failures in this aspect will result in considerable heating.

At present fairly reliable methods have been developed for calculating and modeling these effects. In the development of new designs, extensive use is made of physical scale-modeling of the entire transformer and individual structural components, enabling detection of points of concentration of additional losses at an early stage, so that means can be worked out for avoiding overheating. In designing transformers of maximum power, shunting of massive metal components by stacks of transformer steel and other design features are used to reduce heating.

In connection with the growth of capacities of energy distribution systems in recent years, the problem of dynamic stability of transformers under short-circuit conditions has been especially acute. For a number of years research has been in progress on all major factors that influence dynamic stability: methods of calculation have been improved; new design features have been researched and introduced; improvements have been made in winding manufacture ensuring retention of geometric dimensions after drying; stiffer insulation cardboard with less shrinkage is being used.

At the same time, new structural components are being developed and introduced for pressing the windings of power transformers, ensuring the required force even with some shrinkage of insulation materials. A promising direction is the use of hydraulic jacks, enabling adjustment of pressing of the windings during operation without raising the bell (upper part of the tank).

Simultaneous research is being done on using reinforced wires.

At present, the Ministry of the Electrical Engineering Industry has no special stand for electrodynamic tests of transformers, obviating experiments on this problem. The construction of such a stand is a major problem for the transformer building subsector in the Eleventh Five-Year Plan.

At the present time considerable work is being done on perfecting internal and external cooling of transformers. More precise methods have been developed for temperature calculations of windings with natural and forced circulation of oil through the windings. Transformers of maximum power use mainly directional circulation of oil. Cooling devices of the DTs type have been considerably modified (forced movement of oil through an air-blasted cooler). New coolers have been introduced with low-speed blowers, submerged pumps with shielded stator, and new bimetallic cooling tubes with cut ribbing (to turbulize the airflow). Cooling devices may be either suspended or individually installed. Transformers for large generating facilities chiefly have a water-oil cooling system.

One of the factors that guarantees accident-free operation of transformers is stable up-to-date technology for making components and subassemblies, assembling and drying

FOR OFFICIAL USE ONLY

at the manufacturing plant. Considerable advances have been made in this area in the last 10-15 years.

With the switch to rolled transformer steel there has been a considerable reduction in the labor inputs for making magnetic circuits and an improvement in their quality. Outages involving fire in steel have practically disappeared. This is the result of development and introduction of automatic lines in transformer plants of the subsector for longitudinal and transverse cutting of transformer steel, special stands for assembling and edging magnetic circuits.

A series of machines, lines and fixtures have been developed and to a considerable extent introduced that improve the quality and productivity of labor in manufacture of insulation components and windings. The windings of large transformers are made on vertical winding machines.

Devices have been introduced for axial and radial pressing of windings as they are wound, as well as devices for pressing during drying of windings. This stabilizes the dimensions and density of the winding. A number of lines are used for cutting sheets of cardboard, making piercing racks and spacers. Manufacture of insulating components of complex configuration from celluloid and electrical-grade cardboard has been mastered.

The reliability of high-voltage insulation for oil-filled transformers is determined to a great extent by the quality of drying. Vacuum drying is the conventional method for cellulose insulation. This process has been thoroughly worked out in transformer plants. The vacuum in the drying ovens goes down to 0.1 mm Hg. The conditions for heating up the active part before evacuation have been optimized. A new method of drying in hydrocarbon vapor has now been adopted in Soviet transformer construction. In this technique, the active part of the transformer is heated up by saturated or slightly supersaturated vapor of an organic liquid similar to kerosene at a temperature of 125-140°C with subsequent vacuum drying at a residual pressure of 0.1 mm Hg. The time for drying transformers in hydrocarbon vapor is cut in half, and the quality of drying is improved.

Tests of power transformers are continually being improved for detection of flaws in construction and manufacture.

For purposes of checking the quality of insulation in recent years, tests by commutation pulse have been introduced, as well as protracted (hours-long) testing by voltage on industrial frequency with measurement of the level of partial discharges in insulation.

Work is continuing to perfect protection facilities and methods of troubleshooting transformers during operation. The main protective insulation of high-voltage transformers is the spark-gap arrester. The protective properties of this device are principally what determines and limits the electric effects to which the transformer insulation is subjected. Therefore the improvement of arresters is one of the decisive factors in raising the technical level of the transformers that they protect. Another major protector of oil-filled transformers is the gas relay that has been successfully used for 60 years.

At the present time, all transformers produced in our nation have gas relays made in East Germany, the CEMA nation that specializes in making them.

FOR OFFICIAL USE ONLY

Rubber containers in the expander keep the oil from getting wet and oxidizing. Pointer-type indicators are used for checking the oil level.

New devices are now being developed for keeping track of the condition of transformers during operation. These include a short-circuit counter that accounts for the currents that act on the transformer over a prolonged period, using a special sensor to monitor the temperature of the winding under load with fiberglass optics to transfer the information to an external measuring device.

Among the new facilities for troubleshooting transformers, mention should be made of an acoustic converter of partial discharges. This is a portable instrument that can monitor intensity and determine the point of origin of partial discharges in insulation during factory tests of transformers as well as under operating conditions.

In recent years, a method of spotting initial damages by gases dissolved in the oil has been widely used for troubleshooting transformers. The method is used both by factory testers and operational personnel.

Experience in developing a 667 MVA transformer on 1150 kV, and feasibility studies on transformer equipment with power up to 2000-2400 MVA have shown that a further increase in unit power beyond 1000-1250 MVA will require development of assembly plants with cranes having a hoisting capacity of more than 500 metric tons and the necessary transport facilities. Moreover, the equipment for new superhigh-voltage classes will require an increase in the level of technology and production culture, as well as setting up the necessary test stands at the manufacturing plant.

To realize the prospects of development of transformer construction, and to satisfy the needs of the electric power industry for maximum-power transformer equipment at superhigh voltages, it has been decided to build a new transformer construction shop at Zaporozh'ye Transformer Plant equipped with cranes having a hoisting capacity of up to 1000 metric tons.

The new shop is being designed with a view to making transformers with voltages up to 1800 kVAC and ± 1500 kVDC at unit powers of up to 3000 MVA.

The forthcoming Twenty-Sixth Congress of the CPSU will give new jobs to the energy workers of the nation. The subsector of transformer construction must make its contribution in handling these jobs. Cumulative production experience, the scientific and engineering background and the availability of highly skilled specialists inspire confidence that these problems will find a timely solution.

COPYRIGHT: IZDATEL'STVO "NAUKOVA DUMKA", "TEKHNICHESKAYA ELEKTRODINAMIKA", 1980

6610
CSO: 1861/24

FOR OFFICIAL USE ONLY

INDUSTRIAL TECHNOLOGY

UDC 65.011.56

CLASSIFYING INDUSTRIAL ROBOTS

Moscow O TIPIZATSII PROMYSHLENNYKH ROBOTOV in Russian 1976 (signed to press 21 Jul 76) pp 2, 88

[Annotation and table of contents from book "Classifying Industrial Robots", by Leonid L'vovich Podkaminer, Lyudmila Grigor'yevna Kuznetsova, Nikolay Stepanovich Norkin, Pavel Vasil'yevich Markin, Georgiy Naumovich Rappoport, Levan Kantimirovich Baskayev, Yuriy Viktorovich Solin and Vyacheslav Mikhaylovich Krasnikov, Izdatel'stvo standartov, 10,000 copies, 88 pages]

[Text] The need for using manipulators with programmed control (industrial robots) is currently becoming more and more apparent in many types of plants. However, the capabilities for using manipulator models now under development for large-scale automation is restricted by the fact that they are being designed as individual structures.

In this book, based on systematization of the range of problems covering the field of robotics as a whole, the authors demonstrate the feasibility of classifying industrial manipulators, arranging them in unified-design series, and standardization, which will aid not only in expanding their range of application, but also in simplifying design, shortening development time and reducing cost.

This book is intended for scientists, engineers and technicians. Figures 27, tables 12, references 19.

Contents	page
From the editors	3
Introduction	5
I. Sequence of performance of stages of developing unified-design series of industrial robots	10
II. Structure of automated production sections serviced by robots	13
III. Classification of objects of manipulation and objects of processing by industrial robots	28
IV. Influence that configuration of the automated technological unit has on design of the servicing industrial robot. Classification of industrial robot designs in current use	41
V. Transport robots	60

FOR OFFICIAL USE ONLY

VI. Actuation robots	61
VII. Classifying structural arrangements of systems for controlling individual robots and sections made up of robots	72
VIII. Developing unified-design series of industrial robots	82
References	87

COPYRIGHT: Izdatel'stvo standartov, 1976

6610

CSO: 1861/38

FOR OFFICIAL USE ONLY

NAVIGATION AND GUIDANCE SYSTEMS

UDC 629.7.051

DYNAMICS OF NONLINEAR GYROSCOPIC SYSTEMS

Moscow DINAMIKA Nelineynykh Giroskopicheskikh Sistem in Russian 1981
(signed to press 4 Jan 81) pp 2-6, 223-224

[Annotation, foreword and table of contents from book "Dynamics of Nonlinear Gyroscopic Systems", by Sergey Akimovich Chernikov, Izdatel'stvo "Mashinostroyeniye", 1195 copies, 224 pages]

[Text] Problems of analyzing and synthesizing nonlinear gyroscopic systems of arbitrary order on the basis of frequency methods are explained. The main attention is devoted to exposition of the results of investigating self-excited gyroscopic system oscillations caused by dry friction in cardan suspension axles, play in mechanical transmission, dead zones, limiting and hysteresis in control circuits, etc. The results of investigating the stability of gyroscopic systems with nonlinear elastic and elastic-dissipative coupling are analyzed. Specific examples according to the applied theory of nonlinear oscillations of gyroscopic systems are given.

The book is intended for engineers involved with gyroscopic systems.

Foreword

A great deal of work has been devoted to the solution of nonlinear problems of the dynamics of gyroscopic systems (GS). However, this work is limited either to the framework of precision movement, or to insignificant "smooth" nonlinearities. Neither such nonlinear phenomena as self-excited oscillation nor problems of the stability of significantly nonlinear GS have been treated sufficiently in the literature.

The main direction of the book involves investigation of self-excited oscillation processes caused by the nonlinear nature of the elastic-dissipative coupling in the mechanical part of GS and the nonlinear nature of the amplifying and converting circuit of the control coupline.

FOR OFFICIAL USE ONLY

FOR OFFICIAL USE ONLY

Wide fluctuation of perturbing effects and of GS parameters can cause the excitation of self-sustained oscillations with unacceptable amplitude and frequency which often result in a nonstandard GS operating condition.

Since there is now no general way to determine the asymptotic stability of nonlinear systems as a whole, and since instability is manifested in practice in the form of self-excited oscillations, finding the conditions for self-excited oscillation is one of the basic problems of GS planning. Furthermore, it is necessary to establish both the fact that self-excited oscillations occur and be able to change the parameters of the system, as well as its structure if need be, in order to eliminate the self-excited oscillations or change their parameters in the required direction if a self-excited oscillating condition is standard for the GS. It is important to know how a particular real nonlinearity affects the dynamic properties of the system, how to compensate for the harmful influence of "parasitic" nonlinearities and how best to use the positive properties of nonlinear elements as concomitant as well as specially introduced elements.

In this connection, the problem arises of discovering the general mechanisms by which the influence of various nonlinearities is felt and of developing recommendations to improve dynamics which do not involve specific system parameters or the placement of the nonlinear element within the GS structure.

The basis of the problems which are solved is a dynamic model of a multichannel GS with arbitrary placement of the gyroscopes, which makes it possible to allow for the nonlinear nature of elastic and elastic-dissipative coupling between the kinematic branches and elements of kinematic pairs. In contrast to existing models of nonlinear coupling between elements of a kinematic pair with play, the proposed model allows for omnidirectional properties of the nonlinear branch, the input and output of which change as a function of the state of the energy levels of the parts of the system separated by a gap.

Among nonlinearities, dry friction, which significantly degrades GS accuracy and reliability, deserves special attention. A great deal of work, which is reviewed in detail by N. V. Butenin [11], has been devoted to its influence on the operation of gyroscopic devices. However, most of the work devoted to the influence of friction on GS stability investigates special problems corresponding to the stable region of a nonlinear GS. The natural outcome of these investigations was confirmation of the damping effect of dry friction on a system within the indicated region of the GS phase space. In addition, consideration, e.g., of the inertial properties of an amplifying circuit makes it possible to detect the destabilizing effect of dry friction, i.e., to discover the self-excited oscillation region located within the stability region of a linear system. Furthermore, for GS with dry friction and a doubly astatic driven linear part, there is no stable region, since dry friction unavoidably causes self-excited oscillations.

Another important nonlinear factor which exerts a destabilizing influence on GS, and usually causes self-excited oscillations, is play in mechanical transmissions. The problems associated with investigating the influence of play on the dynamic properties of GS have been far from exhausted, particularly in connection with

FOR OFFICIAL USE ONLY

the inadequacy of the mathematical model of play. The arsenal of methods for suppressing self-excited oscillations is also insufficient. In addition, the influence of other concomitant nonlinearities of passive coupling on the dynamic characteristics of GS with play has been little studied.

Yet another series of important problems of GS dynamics involves nonlinearities of the measurement and amplifier-converter circuit of control coupling with their influence on the stability and precision characteristics of GS, as well as the effect of cross-influence between concomitant nonlinearities of active (control) coupling and passive elastic-dissipative coupling of the mechanical part of a GS. The combined influence of several nonlinearities on the dynamic characteristics of GS has been far from completely studied. Only the first steps have been made in this direction.

The difficulty of the problem is the limited capabilities of existing methods of studying nonlinear systems. Precise methods are valid only for the simplest cases in which the order of the equations does not exceed 2 or 3, and are inapplicable in the case of the complex dynamic model of high-order GS.

The simplest, and sufficiently precise, approximate method is the harmonic linearization method developed by Ye. P. Popov, which has recently become widespread because of its exceptional simplicity and effectiveness [55]. However, a condition for applicability of the harmonic linearization method is filtering properties of the reduced linear part, which are often not satisfied for GS. Examples of GS with an unfiltered linear part are systems with dry friction, systems with tachometric feedback, etc., in which the order of the numerator of the reduced linear part is less only by unity than the order of the denominator, as well as systems with clearly defined resonance properties and low-frequency (pre-resonant) periodic conditions. The formal application of the harmonic linearization method in these cases may yield quantitative errors and even qualitatively incorrect results [51, 96, 97]. In addition, a special type of periodic movement--so-called slippage or stop motion--caused by jumps in the derivatives of the argument of the nonlinear function is characteristic for GS with dry friction. The presence of jumps at the input of the nonlinear element makes it unjustified to apply the harmonic linearization method to the investigation of periodic solutions, if only because the form of the oscillations is significantly nonsinusoidal. In connection with this, one of the chapters (the third in the present book) is devoted to developing a method for investigating nonlinear systems with an unfiltered linear part which can be used to conduct qualitative investigations of distinct types of periodic conditions--slipping, partially slipping and self-sustained oscillating conditions with stop--which are not subject to investigation using the first harmonic method, and to investigate periodic modes in critical cases of low oscillation amplitude to which the applicability conditions of the harmonic linearization method do not extend, being based on estimating the sensitivity of a periodic solution to higher harmonics and small parameters.

Finally, the problem of increasing the precision characteristics of GS is inseparably associated with the problem of damping their oscillations which, as we know, consists of the incompatible requirements of high static and dynamic

FOR OFFICIAL USE ONLY

FOR OFFICIAL USE ONLY

accuracy on the one hand, and stability on the other. Furthermore, increasing the damping moments with respect to cardan suspension axles and improving the stability of GS simultaneously degrades its constrained motion characteristics. The elastic compliance of construction elements further exacerbates this problem, since additional resonant frequencies appear. Furthermore, if these resonant frequencies are close to one another, it is extremely difficult to provide good stabilization throughout the entire frequency range with the help of linear correcting devices in the feedback circuit. The problem of synthesizing nonlinear correcting couplings which improve the dynamic properties of the system arises in this connection.

The book also considers control processes in GS in which a self-excited oscillation condition is normal.

Problems of nonlinear dynamics of GS are solved in the book on the basis of frequency methods, particularly the harmonic linearization method, which have recommended themselves in engineering practice.

The book is based on the author's work on the dynamics of nonlinear GS [83, 86, 97].

Table of Contents

Foreword	3
Chapter 1. Equations of nonlinear gyrosystems and dynamic models of nonlinear coupling	7
1.1. Motion equations of GS with nonlinear coupling	7
1.2. Nonlinear models of dissipative coupling	13
1.3. Nonlinear models of elastic and elastic-dissipative coupling	16
1.4. Models of coupling with play	18
1.5. Generalized model of nonlinear coupling	23
Chapter 2. Frequency characteristics of reduced linear parts of GS with nonlinear coupling	27
2.1. Linear GS motion equations	27
2.2. Frequency characteristics of reduced linear parts of GS with "external" nonlinear coupling (unidimensional nonlinear GS)	31
2.3. Frequency characteristics of reduced linear parts of GS with internal nonlinear coupling (two-dimensional nonlinear GS)	38
2.4. Characteristics of reduced linear parts of GS with active nonlinear coupling	48
Chapter 3. Method of investigating nonlinear gyrosystems with unfiltered linear part	53
3.1. Periodic modes in nonlinear gyrosystems. "Jump" equations	53
3.2. Affine-equivalent conversions of nonlinear systems	57
3.3. Unification of nonlinear structure	65
3.4. Harmonic linearization of dynamic nonlinear sections	69
3.5. Harmonic linearization of relay-controlled dynamic sections	78

FOR OFFICIAL USE ONLY

Chapter 4. Self-excited oscillations of GS with nonlinear dissipative coupling	85
4.1. Destabilizing effect of friction. Qualitative analysis	85
4.2. Determination of parameters of relay-controlled periodic modes. Isolation of stability region	94
4.3. Relayed self-excited oscillations of GS with external nonlinear dissipative coupling	98
4.4. Relayed self-excited oscillations of GS with internal nonlinear dissipative coupling	109
4.5. Allowance for higher harmonics and jumps of relayed self-excited oscillations of GS with dry friction	114
Chapter 5. Relayed-slipping self-excited oscillations and stability of GS with dry friction	127
5.1. Characteristics of converted equivalent linear parts of GS with nonlinear friction	127
5.2. Determination of parameters of relayed-slipping periodic modes. Isolation of stability regions	131
5.3. Relayed-slipping self-excited oscillations of GS with dry friction	142
Chapter 6. Self-excited oscillations of GS with play and nonlinear elastic-dissipative coupling	151
6.1. Self-excited oscillations and stability of GS with nonlinear elastic coupling	152
6.2. Self-excited oscillations and stability of GS with nonlinear elastic-dissipative coupling	162
6.3. Determination of parameters of self-excited oscillations of GS with nonlinear elastic coupling in case of unfiltered linear part	169
6.4. Asymmetrical self-excited oscillations and stability of GS with nonlinear elastic coupling with external perturbation	173
Chapter 7. Self-excited oscillations of gyrosystems with concomitant nonlinearities of control circuits	185
7.1. Influence of concomitant nonlinearities of orthogonal control circuits	185
7.2. Influence of concomitant nonlinearities of local control circuit	193
Chapter 8. Damping of self-excited oscillations	196
8.1. Damping of self-excited oscillations of GS with play using forces of dry friction	196
8.2. Damping effect of concomitant nonlinearities in control circuits	206
8.3. Nonlinear active damping	209
A. Nonlinear control	209
B. Nonlinear correction	211

FOR OFFICIAL USE ONLY

8.4. Correction of static characteristics on nonlinear coupling	212
8.5. Inertial damping of GS oscillations	214
References	219

COPYRIGHT: Izdatel'stvo "Mashinostroyeniye", 1981

6900

CSO: 1861/36

FOR OFFICIAL USE ONLY

FOR OFFICIAL USE ONLY

UDC 531.383

PROGRAMMED ANGULAR MOVEMENTS OF GYROSTAT WHEN QUATERNIONS ARE USED TO DETERMINE ITS ORIENTATION

Kiev PRIKLADNAYA MEKhanika in Russian Vol 17, No 5, May 81 (manuscript received 18 Feb 80) pp 113-116

[Article by A. Ye. Zakrzhevskiy, Institute of Mechanics, UkSSR Academy of Sciences, Kiev]

[Text] The problem of setting up programmed motions of a controlled object about its center of mass is currently of considerable practical interest in connection with the intensive development of modern technology. Resolution of this problem involves either construction or closure of a system of equations of motion control with respect to a given special solution (Ref. 1, 2]. The stability of such solutions can be ensured by constructing a stabilization system that is optimum in some sense [Ref. 4, 5, 6].

The use of Euler-Krylov angles for determining the orientation of a solid in space precludes the creation of a non-Cardan orientation system based on integrating the equations of motion. This is due to degeneration of kinematic equations at certain values of the angles of orientation. The use of direction cosines leads to a considerable increase in the order of the system of the equations of motion. In such a case it is most convenient to use quaternions, and specifically Rodrigues-Hamilton parameters [Ref. 1] as the orientation parameters.

Let us consider a method of producing stable programmed motions about the center of mass of a solid moving in a central force field. We will take the Rodrigues-Hamilton parameters as the orientation parameters. In this way when angular velocity sensors and computers are available we can create a mathematical "platform" as a result of integrating nondegenerate kinematic equations. The actuating elements of the control system are three one-degree gyroscopes with axes lying along the principal axes of inertia of the entire system.

Let us introduce the following coordinate systems as shown in the diagram: inertial $CX_1X_2X_3$, principal central $Ox_1x_2x_3$ fixed to the solid, orbital $Ox_1^0Px_2^0Px_3^0P$, and the system of axes $O\xi_1\xi_2\xi_3$ in translational motion along the orbit.

We will describe the dynamics of the object by the following equations: equations of motion in the form of three dynamic Euler's equations

FOR OFFICIAL USE ONLY

$$C_1 \dot{\omega}_1 + (C_3 - C_2) \omega_2 \omega_3 + \dot{H}_1 + \omega_2 H_3 - \omega_3 H_2 = m_1 \quad (1 \ 2 \ 3); \quad (1)$$

kinematic equations

$$\begin{aligned} 2\dot{\lambda}_0 &= -\omega_1 \lambda_1 - \omega_2 \lambda_2 - \omega_3 \lambda_3; & 2\dot{\lambda}_1 &= \omega_1 \lambda_0 + \omega_3 \lambda_2 - \omega_2 \lambda_3; \\ 2\dot{\lambda}_2 &= \omega_2 \lambda_0 + \omega_1 \lambda_3 - \omega_3 \lambda_1; & 2\dot{\lambda}_3 &= \omega_3 \lambda_0 + \omega_2 \lambda_1 - \omega_1 \lambda_2; \end{aligned} \quad (2)$$

equations of motion of one-degree gyroscopes

$$\dot{H}_i = -I_i \dot{\omega}_i - \tau_i H_i + U_i \quad (i = 1, 2, 3). \quad (3)$$

Here the C_i are the principal moments of inertia of the carrier body with braked gyroscope rotors, ω_i are the angular velocities of the carrier body, H_i are the absolute values of the vectors of kinetic moments of the gyroscopes in their rotation about their own axes; λ_i are the Rodrigues-Hamilton parameters that determine orientation of the fixed system of axes relative to basis $O\xi_1\xi_2\xi_3$, τ_i are the coefficients of friction in the gyroscope axes, U_i are the controlling torques, m_i are the external moments of the central force field, (123) denotes that the other two equations (1) can be obtained by cyclic permutation of subscripts. System of equations (1)-(3) has one first integral

$$\lambda_0^2 + \lambda_1^2 + \lambda_2^2 + \lambda_3^2 = 1. \quad (4)$$

Let us consider the problem of constructing an algorithm of formation of controlling torques U_i to ensure stable execution of programmed spatial movements by the carrier body

$$\lambda_i = \mu_i(t); \quad t \in [t_0, T] \quad (i = 1, 2, 3). \quad (5)$$

In contrast to Ref. 3, no constraints are imposed on factor μ_1 .

The formulated problem reduces to closure of a system of equations of motion by control with respect to a given special solution [Ref. 7]. As a result of its solution we find the programmed control U_i ($i = 1, 2, 3$).

Let us combine the unit vectors \bar{i}_k of the hypercomplex space of quaternions with basis $O\xi_1\xi_2\xi_3$. The fixed axes are put into one-to-one correspondence with unit vectors e_k , the orbital axes--with e_k^{OP} , and axes $CX_1X_2X_3$ --with \bar{e}_k^C . Let us introduce normalized proper quaternions of transformation of the bases [Ref. 1]

$$\bar{c}_h = \Lambda \bar{i}_h \Lambda; \quad \bar{c}_k^C = N \bar{i}_k^C \bar{N}, \quad \bar{c}_h^{OP} = P \bar{i}_h^{OP} \bar{P}, \quad (6)$$

where the tilde denotes a quaternion conjugate with the initial one, the small circle corresponds to the operation of multiplication defined by quaternion algebra.

In the process of construction of quaternions that assign the operation of rotation of the bases, it may become necessary to express their components in terms of direction cosines. If basis E relative to basis I is defined by a matrix of direction cosines A, then the parameters of quaternion A that defines rotation of basis I to coincidence with E have the form [Ref. 1]

FOR OFFICIAL USE ONLY

FOR OFFICIAL USE ONLY

$$\lambda_0 = \pm \frac{\sqrt{1 + \text{Sp } A}}{2}; \quad \lambda_1 = \pm \frac{a_{33} - a_{32}}{4\lambda_0};$$

$$[\lambda_2 = \pm \frac{a_{31} - a_{13}}{4\lambda_0}; \quad \lambda_3 = \pm \frac{a_{12} - a_{21}}{4\lambda_0},$$

where $\text{Sp } A = \sum_{i=1}^3 a_{ii}$, the sign preceding the expressions to be taken the same for all λ_i .

Assuming an undisturbed orbit, and consequently an unperturbed kinetic moment in migratory motion, we can write

$$\frac{d\bar{K}}{dt} = \bar{m} = \frac{3\mu}{r^3} \bar{k} \times \Theta^0 \cdot \bar{k}, \quad (7)$$

where \bar{K} is the kinetic moment of the system in its motion relative to center of mass 0, \bar{m} is the moment of external forces relative to the center of mass, μ is the gravitational constant, r is the radius of the orbit, \bar{k} is the unit vector of direction \overline{CO} , Θ^0 is the tensor of inertia of the solid with braked gyroscope rotors.

The overall kinetic moment in relative motion is written as

$$\bar{K} = \bar{\omega} \cdot \Theta^0 + \sum_{k=1}^3 H_k \bar{e}_k. \quad (8)$$

Let $\lambda_i = \mu_i^0$ ($i = 0, \dots, 3$), $\omega_k = q_k^0$, $\bar{e}_k = \bar{e}_k^0$ ($k = 1, 2, 3$) at $t = t_0$. The initial kinetic moment takes the form

$$\bar{K}_0 = \sum_{k=1}^3 (H_{k0} + C_k q_k^0) \bar{e}_k^0. \quad (9)$$

To transform the components of these vector quantities, we introduce quaternions comprised of the components of these vectors in bases I, E, E^{OP}

$$\bar{m}^I = \sum_{k=1}^3 m_k^I \bar{i}_k; \quad \bar{m}^E = \sum_{k=1}^3 m_k^E \bar{i}_k; \quad \bar{k}^{I,OP} = \sum_{j=1}^3 k_j^{E,OP} \bar{i}_j.$$

Here the \bar{i}_k are unit vectors of the hypercomplex space of quaternions that formally coincide with the unit vectors of basis $O\xi_1\xi_2\xi_3$, which for angular displacements is inertial.

Using the introduced rotational transformations (6), let us determine the components of vector equation (7) in the inertial coordinate system. Since $k = e^{\Theta^0 P}$, then $\bar{k}^I = P \bar{e}_k^0 P^{-1}$; $\bar{k}^E = M P \bar{e}_k^0 P^{-1} M^{-1}$. As a result, projections \bar{m} on the fixed basis are determined, and quaternion \bar{m}^E is constructed. In virtue of (6), we have $\bar{m}^I = M \bar{m}^E M^{-1}$; $K_0^I = M_0 K_0^{I,OP} M_0^{-1}$, where quaternion M is determined by components $\mu_i(t)$, and M_0 is determined by components μ_i^0 ($i = 0, 1, 2, 3$).

Let us write (7) in the inertial basis and integrate

$$\bar{K}^I(t) = \bar{K}_0^I + \int_{t_0}^t \bar{m}^I(\tau) d\tau.$$

FOR OFFICIAL USE ONLY

FOR OFFICIAL USE ONLY

Converting to the fixed axes, with consideration of (8) we get

$$\bar{K}^E = \bar{M} \circ \bar{K}' \circ \bar{M} = \bar{M} \circ (\bar{H}' + K_T') \circ \bar{M}.$$

Whence

$$\bar{H}^E = \bar{M} \circ \bar{K}' \circ \bar{M} - \bar{K}_T^E \left(\bar{K}_T^E = \sum_{k=1}^3 C_k q_k \bar{i}_k \right). \quad (10)$$

Using the derivative that has been formally introduced into the quaternion apparatus [Ref. 1], and considering that $\bar{M} \circ \bar{K}' \circ \bar{M} = \bar{m}^E$, with consideration of kinematic equations (2) for programmed motion of a solid in form $\bar{M} = \bar{M} \circ \bar{q}^E$, we get

$$\dot{\bar{H}}^E = \frac{1}{2} (\bar{M} \circ \bar{q}^E \circ \bar{K}' \circ \bar{M} + \bar{M} \circ \bar{K}' \circ \bar{M} \circ \bar{q}^E) - \bar{K}_T^E + \bar{m}^E.$$

As a result we construct the programmed controlling moment

$$U_k = \dot{H}_k + I_k \dot{q}_k + \tau_k H_k \quad (k = 1, 2, 3), \quad (11)$$

The problem of stabilization of the resultant programmed motions should be solved on the basis of ensuring a given quality of transient processes.

Let us turn to analytical design of an optimum regulator with respect to the criterion of generalized work [Ref. 4]. This method enables us to get a solution in closed form for the problem of optimum stabilization for the complete system of nonlinear equations of motion of the object, closed by control, in perturbations. Such a capability is due to the fact that the second members of the equations of motion in perturbations, written in normal Cauchy form, are polynomials with a finite number of terms.

Actually, the equations in perturbations for (1)-(3) take the form

$$\dot{x}_i = \sum_{j=1}^{10} a_{ij} x_j + \sum_{k,j=1}^{10} a_{ijk} x_j x_k + \sum_{j=1}^3 b_{ij} u_j, \quad (12)$$

where a_{ij} , a_{ijk} , b_{ij} are known functions of time defined by the programmed law of motion.

Solution of the problem of optimum stabilization reduces to solution of the Cauchy problem for the Riccati system of matrix equations, the order being 50. The controls $u_j = u_j(x_1, \dots, x_{10})$ ($j = 1, 2, 3$) that are constructed as a result should be summed with programmed controlling moments $U_j = U_j^0 + u_j$ ($j = 1, 2, 3$), the u_j being homogeneous functions of perturbations of phase variables, and consequently vanishing on special solution (5).

Construction of optimum stabilization by the proposed method guarantees existence of a positively defined function that satisfies the conditions of the Lyapunov theorem of motion stability.

Thus the use of Rodrigues-Hamilton parameters enables us to create a mathematical "platform" for determining the orientation of a solid in space, based on numerical

FOR OFFICIAL USE ONLY

integration of nondegenerate kinematic equations, and yields a solution in closed form for the problem of optimum stabilization of programmed motions.

REFERENCES

1. Branets, V. N., Shmyglevskiy, I. P., "Primeneniye kvaternionov v zadachakh oriyentatsii tverdogo tela" [Using Quaternions in Problems of Orientation of a Solid], Moscow, Nauka, 1973, 320 pp.
2. Yerugin, N. P., "Construction of the Entire Set of Systems of Differential Equations That Have a Predetermined Integral Curve", PRIKLADNAYA MATEMATIKA I MEKHANIKA, Vol 16, No 6, 1952, pp 659-670.
3. Zakrzhevskiy, A. Ye., "Programmed Control of Angular Motion of Gyrostat in Central Force Field", PRIKLADNAYA MEKHANIKA, Vol 15, No 5, 1979, pp 85-91.
4. Krasovskiy, A. A., "Sistemy avtomaticheskogo upravleniya poletom i ikh analiticheskoye modelirovaniye" [Automatic Flight Control Systems and Their Analytical Modeling], Moscow, Nauka, 1973, 558 pp.
5. Krasovskiy, N. N., "Teoriya upravleniya dvizheniyem" [Theory of Motion Control], Moscow, Nauka, 1968, 476 pp.
6. Letov, A. M., "Dinamika poleta i upravleniye" [Flight Dynamics and Control], Moscow, Nauka, 1969, 360 pp.
7. Galiullin, A. S., Mukhametzyanov, I. A., Mukharlyamov, R. G., Furasov, V. D., "Postroyeniye sistem programmogo dvizheniya" [Construction of Programmed Control Systems], Moscow, Nauka, 1971, 352 pp.

COPYRIGHT: Izdatel'stvo "Naukova dumka", "Prikladnaya mekhanika", 1981

6610

CSO: 8144/089

FOR OFFICIAL USE ONLY

FOR OFFICIAL USE ONLY

UDC 531.38

INVERSE PROBLEM OF GYROINERTIAL MEASUREMENT SYSTEMS

Kiev PRIKLADNAYA MEKHANIKA in Russian Vol 17, No 5, May 81 (manuscript received 31 Jul 79) pp 106-112

[Article by F. M. Zakharin and M. A. Kharitonov, Kiev Higher Military Aviation Engineering Academy]

[Text] The problem of determining angular velocity, linear acceleration and other motion parameters of a base from the output signals of gyroinertial indicators can be treated as the inverse problem of gyroinertial measurement systems. The conventional approach to solution of the inverse problem of gyroinertial measurement systems [Ref. 6] that assumes utilization of the inverse equations of gyroinertial measurement systems requires verification of conditions of stability and applicability in accordance with D. R. Merkin for the solutions of these equations, and also exact assignment of the initial values of the parameters to be determined. In this paper, an approach to solution of the inverse problem of gyroinertial measurement systems is proposed that is based on optimum estimation theory.

1. Consider a gyroinertial measurement system installed on a moving base and containing N indicators (gyroscopes, accelerometers). The location of each indicator with respect to coordinate system $Ox_1x_2x_3$ fixed to the base is determined by radius vector \vec{r}_n and rotational matrix $B_n = \|b_{ij}\|^n$ ($n=1, 2, \dots, N$). The equations that describe motion of an arbitrary system of this kind [Ref. 6] are represented in general form

$$\dot{q} = f(q, x, \dot{x}, \gamma, t) + \xi(t), \quad (1.1)$$

where $q = (q_0^T, q_0^T)^T$; $q_0 = (q_1^1, \dots, q_{s_1}^1, q_1^2, \dots, q_{s_2}^2, \dots, q_1^N, \dots, q_{s_N}^N)^T$ is the vector of generalized coordinates of sensing elements of the indicators, s_i ($i=1, 2, \dots, N$) is the number of generalized coordinates of the sensing element of the i -th indicator, $x = (\omega_1, \omega_2, \omega_3, w_1, w_2, w_3)^T$ is a vector made up of projections of the absolute angular velocity of the base (ω_1) and apparent acceleration (w_1) of point O on the axes of coordinate system $Ox_1x_2x_3$, $\gamma = (\gamma_1^T, \gamma_2^T, \dots, \gamma_N^T)^T$; γ_i is the vector of parameters of the i -th indicator such as mass of the sensing element, moments of inertia, coefficients of imbalance, unequal stiffness, damping, components of \vec{r}_n and B^n and so on, $\xi(t)$ is the vector of random perturbations, the superscript T is the transpose symbol, and the dot indicates differentiation with respect to time.

In some cases, the a priori information on properties of the function $x(t)$ can be used to construct the model

FOR OFFICIAL USE ONLY

FOR OFFICIAL USE ONLY

$$\dot{x}_1 = f_{x_1}(x_1) + \xi_{x_1}(t), \quad (1.2)$$

where $x_1 = (x_1^T, (dx/dt)^T, \dots, (d^m x/dt^m)^T)^T$; $f_{x_1}(x_1)$ is a known vector function, ξ_{x_1} is a random vector with known statistic.

Combining equations (1.1) and (1.2), we get a system of the form

$$x_2 = f_{x_2}(x_2, \gamma) + \xi_{x_2}(t), \quad (1.3)$$

where

$$\xi_{x_2} = (\xi_{x_2}^T, \xi_{\dot{x}_2}^T)^T; \quad x_2 = (x_1^T, \dot{x}_1^T)^T.$$

Usually the output signals of gyroinertial indicators are known functions of the generalized coordinates of the sensing element and parameters γ measured with errors

$$y = h(x_2, \gamma) + \zeta(t), \quad (1.4)$$

where $\zeta(t)$ is the vector of random measurement errors.

The problem of estimating the vector of state $x_2(t)$ of system (1.3), (1.4) is a standard problem of nonlinear filtration [Ref. 8]. If we assume that $h = q_0$ and \dot{q}_0 , \ddot{q}_0 are negligibly small (or their values are measured), while the dimensionality of q_0 is not less than that of the vector $x_3 = (x^T, \dot{x}^T)^T$, then on the basis of (1.1) we can get a nonlinear regression model of the form

$$z = g(x_3, \gamma) + \xi_{x_3}(t). \quad (1.5)$$

An algorithm for estimating vector x_3 from observed vector z is to be found in particular in Ref. 1.

2. Consider a gyroinertial measurement system made up of two unbalanced electrostatic gyroscopes. With consideration of Ref. 2, 3, the averaged equations that describe the motion of an aspherical unbalanced rotor of an electrostatic gyroscope in a suspension with unequal stiffness at small nutation angle $\theta(t)$ is represented as

$$\dot{a}_{31} = \omega_3^* a_{32} - \omega_2^* a_{33} \quad (1 \ 2 \ 3); \quad \dot{K} = \frac{E \cos \beta}{2} \sum_{i=1}^3 (1 - a_{3i}^2) \beta_i(\omega_{0i}); \quad (2.1)$$

$$\dot{\theta} = \theta \frac{E}{K} \sum_{i=1}^3 \{ \beta_i(\omega_{0i}) \cos^2 \beta - 2\beta_i(\omega_{02}) \sin^2 \beta - [\beta_i(\omega_{01}) \cos^2 \beta - 2\beta_i(\omega_{02}) \sin^2 \beta - 2\beta_i(\omega_{03}) \cos^2 \beta] a_{3i}^2 \}.$$

Here

$$\omega_i^* = \tilde{\omega}_i + \Lambda \omega_i; \quad \tilde{\omega}_i = \sum_{k=1}^3 b_{ik} \omega_k; \quad \tilde{\omega}_i = \sum_{k=1}^3 b_{ik} \omega_k; \quad (i=1, 2, 3);$$

$$\Lambda \omega_1 = \frac{1}{K} \left\{ m E \sin \beta \tilde{\omega}_1 + \frac{(E \cos \beta)^2}{2} m [\alpha_1(\omega_{01}) a_{31} + (\beta_2(\omega_{01}) - \right.$$

$$\left. \beta_3(\omega_{01})) a_{32} a_{33} \right] - a_0 \sum_{n=1}^N \alpha_n \alpha_n^T \right\} \quad (1 \ 2 \ 3); \quad \alpha_i(\omega_{0h}) = -\omega_{0h}^2 \gamma_i(\omega_{0h});$$

FOR OFFICIAL USE ONLY

FOR OFFICIAL USE ONLY

$$\begin{aligned}
v_i(\omega_{0k}) &= \operatorname{Re} v_i(j\omega_{0k}); & \beta_i(\omega_{0k}) &= -\omega_{0k}^2 \mu_i(\omega_{0k}); & \mu_i(\omega_{0k}) &= \operatorname{Im} v_i(j\omega_{0k}); \\
v_i(D_i) &= Q_i(D_i) [Q_i(D_i) + mD_i^2]^{-1}; & Q_i(D_i) &= Q_i^0 A_i(D_i)/B_i(D_i); \\
D_i &= d/dt; & j &= \sqrt{-1} \quad (i=1, 2, 3); & \omega_{01} &= \omega_0(1+\kappa-\kappa_*); \\
\omega_{03} &= \omega_0\kappa_*; & \omega_0 &= K/I_3; & \omega_{02} &= \omega_0(1+\kappa); & \omega_{04} &= \omega_0(1+\kappa+\kappa_*); \\
\kappa_* &= \kappa \cos \theta; & \phi_n &= M_{2n} \left[E_{2n} \left(1 + k_{2n} \sum_{k=1}^3 A_k^n \tilde{\omega}_k \right) \right]^2 + \\
&+ M_{2n-1} \left[E_{2n-1} \left(1 - k_{2n-1} \sum_{k=1}^3 A_k^n \tilde{\omega}_k \right) \right]^2; & A_k^n &= \alpha_k^n m [Q_k^0]^{-1}; \\
a_0 &= \frac{\pi}{2} e_0 r_1^2; & e_0 &= 8.85 \cdot 10^{-12} \text{ KJ}^2/\text{H} \cdot \text{M}^2; & (k=1, 2, 3); & M_v &= \sum_{l=1}^L e_{2l} I_{2l}^v; \\
I_{2l}^v &= I_{2l-2}^v + J_l^v; & J_l^v &= \frac{4l-1}{l} [P_{2l}^v(\tilde{\alpha}_3^n) \int_{\cos \psi_1^v}^{\cos \psi_2^v} z P_{2l-1}(z) dz - \\
&- \tilde{\alpha}_3^n P_{2l-1}^v(\tilde{\alpha}_3^n) \int_{\cos \psi_1^v}^{\cos \psi_2^v} P_{2l-2}(z) dz]; & \tilde{\alpha}_3^n &= \sum_{i=1}^3 \alpha_i^n a_{3i}; & v &= 2n-1, 2n; \\
&(n=1, 2, \dots, N);
\end{aligned}$$

$A = \|a_{ij}\|$ is the orientational matrix of coordinate system ξ_1, ξ_2, ξ_3 fixed to the housing of the electrostatic gyroscope with respect to coordinate system $\zeta_1, \zeta_2, \zeta_3$ fixed to the vector of kinetic moment K [Ref. 2], $B = \|b_{ij}\|$ is the matrix of orientation of coordinate system $\xi_1 \xi_2 \xi_3$ relative to $Ox_1 x_2 x_3$, $\tilde{\omega}_1, \tilde{\omega}_2$ are projections of vectors ω and w on axes $\xi_1 \xi_2 \xi_3$, $I_3 = I_1(1+\kappa)$, I_1 are the polar and equatorial moments of inertia of the rotor, $Q_i(D_i)$ is the transfer function of the i -th channel of the three-channel tracking system of the suspension, equivalent in force formation to the initial N -channel system, r_1, r_2 are the nominal radii of the rotor and casing of the electrostatic gyroscope, E_v is field strength under the v -th electrode in the absence of rotor displacement, k_v is the gain of the tracking system of the suspension, e_{2l} are the coefficients of the expansion of the function that describes the surface of the rotor with respect to Legendre polynomials P_{2l} ; ψ_1^v, ψ_2^v are angles that determine the shape of the v -th electrode [Ref. 3], ϵ_0 is the [di]electric constant, α_i^n ($i=1, 2, 3$) are the direction cosines of the axis of sensitivity of the n -th channel of the tracking system of the suspension in coordinate system $\xi_1 \xi_2 \xi_3$, m is the mass of the rotor, (123) denotes that the two other relations are obtained from the given one by cyclic permutation of subscripts, $P_r^i(u) = dP_r(u)/du$.

The first-approximation equations that define linear displacements of the rotor of the electrostatic gyroscope relative to the casing take the form

$$D_t^2 R_t = m w_t + F_t; \quad F_t = -A^T Q(D_t) A (R_t + E_t). \quad (2.3)$$

FOR OFFICIAL USE ONLY

FOR OFFICIAL USE ONLY

Whence

$$R_{\xi} = -B_0 E_{\xi} + Q_0^{-1} m \omega_{\xi}; \quad y \stackrel{\Delta}{=} R_{\xi} + E_{\xi} = A(R_{\xi} + E_{\xi}) = \\ = [I - V(D_i)] E_{\xi} + \frac{m \omega_{\xi}}{Q_0}. \quad (2.4)$$

Here

$$B_0 = A^T V(D_i) A; \quad Q(D_i) = \text{diag}\{Q_i\}; \quad Q_0 = \text{diag}\{Q_i^0\}; \\ V(D_i) = \text{diag}\{v_i(D_i)\}; \quad I = \text{diag}\{1\}; \quad E_{\xi} = \frac{E \cos \beta}{2} [(1 + \cos \theta) \times \\ \times \cos(\psi + \varphi) + (1 - \cos \theta) \cos(\psi - \varphi)] + E \sin \beta \sin \psi \sin \theta; \quad (2.5) \\ E_{\xi} = \frac{E \cos \beta}{2} [(1 + \cos \theta) \sin(\psi + \varphi) + (1 - \cos \theta) \sin(\psi - \varphi)] - \\ - E \sin \beta \cos \psi \sin \theta; \quad E_{\xi} = E (\cos \beta \sin \theta \sin \varphi + \sin \beta \cos \theta); \quad \psi = K H_1^{-1}; \\ v = K \kappa (1 + \kappa)^{-1} \cos \theta H_1^{-1}; \quad \varphi = -\nu t;$$

ψ, ϕ are angles of precession and proper rotation [Ref. 2]. The subscripts of the expression ξ_i, ζ_i indicate the coordinate system in which the given vector is considered.

Substituting (2.5) in (2.4) after a number of transformations we get

$$y_i = \{[a_{1i} A_i(\omega_{01}) - a_{2i} B_i(\omega_{01})] \cos \omega_{01} t + [a_{2i} A_i(\omega_{01}) + a_{1i} B_i(\omega_{01})] \times \\ \times \sin \omega_{01} t\} \frac{1 + \cos \theta}{2} + \{[a_{1i} A_i(\omega_{04}) - a_{2i} B_i(\omega_{04})] \cos \omega_{04} t + [a_{2i} A_i(\omega_{04}) + \\ + a_{1i} B_i(\omega_{04})] \sin \omega_{04} t\} \frac{1 - \cos \theta}{2} + \{[-a_{2i} A_i(\omega_{02}) - a_{1i} B_i(\omega_{02})] \cos \omega_{02} t + \\ + [a_{1i} A_i(\omega_{02}) - a_{2i} B_i(\omega_{02})] \sin \omega_{02} t\} \sin \theta \lg \beta - \{a_{3i} (B_i(\omega_{03}) \cos \omega_{03} t - \\ - A_i(\omega_{03}) \sin \omega_{03} t)\} \sin \theta + m \omega_i [Q_i^0]^{-1} \quad (i = 1, 2, 3), \quad (2.6)$$

where

$$A_i(\omega_{0h}) = E \cos \beta (1 - \gamma_i(\omega_{0h})); \quad B_i(\omega_{0h}) = E \cos \beta \mu_i(\omega_{0h}) \quad (i = 1, 2, 3; \\ k = 1, 2, 3, 4). \quad (2.7)$$

Assuming that $K \cong \text{const}$, $\theta \rightarrow 0$, in place of (2.6) we find

$$y_i = [a_{1i} A_i(\omega_0) - a_{2i} B_i(\omega_0)] \cos \omega_0 t + [a_{2i} A_i(\omega_0) + a_{1i} B_i(\omega_0)] \sin \omega_0 t + \\ + m \omega_i [Q_i^0]^{-1} \quad (i = 1, 2, 3). \quad (2.8)$$

3. Let us assume that there are l sensors of linear displacements of the rotor [Ref. 7] with output signals represented in the form

$$z_i = \sum_{k=1}^3 \lambda_{ki}^t \xi_k \quad (i = 1, 2, \dots, l), \quad (3.1)$$

where λ_{ki}^t ($k = 1, 2, 3$) are direction cosines of the axis of sensitivity of the i -th sensor in coordinate system $\xi_1 \xi_2 \xi_3$.

FOR OFFICIAL USE ONLY

FOR OFFICIAL USE ONLY

Let us consider the problem of reconstructing the instantaneous values of projections of the apparent acceleration w_i and absolute angular velocity ω_i , and also the direction cosines d_{ij} of coordinate system $Ox_1x_2x_3$ relative to inertial basis $i_1i_2i_3$ associated with the vectors of kinetic moments of the electrostatic gyroscope at the initial instant $t=t_0$ ("true" direction cosines) from observations $z_i(t)$ ($i=1, 2, \dots, l$). In the general case this problem reduces to a problem of non-linear filtration for a system described by equations of form (1.2), Poisson equations for matrix $D = \|d_{ij}\|$, and also equations of form (2.1) and relations (3.1) for both gyroscopes.

A simpler scheme for solving the investigated inverse problem involves the following operations:

- 1) obtaining preliminary estimates of components of the apparent acceleration w_i and the direction cosines of the vectors of kinetic moments a_{ji}^0 ($n=1, 2$) (n is the number of the electrostatic gyroscope);
- 2) compensating the drift of the electrostatic gyroscope and constructing a preliminary estimate of the matrix of "negative" direction cosines $D = \|d_{ij}\|$ [Ref. 9];
- 3) smoothing the preliminary estimates of projections of the apparent acceleration and the "true" direction cosines, and estimating the projections of absolute angular velocity.

If instantaneous values of the output signals $z_j(t)$ ($j=1, 2, \dots, l$) are observed at times $t_n = t_{n-1} + \Delta t$ ($n=2, 3, 4; \Delta t = \frac{\pi}{2\omega_0}$), then with consideration of the smallness of Δt for estimate \tilde{w}_i and a_{3i} ($i=1, 2, 3$), we can use the following algorithm. We represent relations (2.8) in the form

$$z_j(t_n) = \sum_{v=1}^3 \lambda_{vj} y_v(t_n) \quad (n=1, 2, 3, 4), \quad (3.2)$$

where

$$y_v(t_n) = y_{1v} + y_{2v} \cos \omega_0 t_n + y_{3v} \sin \omega_0 t_n; \quad y_{1v} = m\omega_v [Q_v^0]^{-1}; \\ y_{2v} = A_v a_{1v} - B_v a_{2v}; \quad y_{3v} = A_v a_{2v} + B_v a_{1v} \quad (v=1, 2, 3).$$

Then

$$z(t_n) = \Phi_0(t_n) y(t_n); \quad y(t_n) = \Phi_0^+ z(t_n). \quad (3.3)$$

Here

$$z(t_n) = (z_1(t_n), z_2(t_n), \dots, z_l(t_n))^T; \quad y(t_n) = (y_1(t_n), y_2(t_n), y_3(t_n))^T.$$

Considering that

$$y_i(t_n) = y_{1i} + y_{2i} \cos \omega_0 t_n + y_{3i} \sin \omega_0 t_n; \quad t_n = t_{n-1} + \frac{\pi}{2\omega_0} \quad (n=2, 3, 4), \quad (3.4)$$

FOR OFFICIAL USE ONLY

FOR OFFICIAL USE ONLY

we can easily get the relations

$$\tilde{u}_i = Q_i^0 m^{-1} \tilde{y}_i \quad (i = 1, 2, 3); \quad (3.5)$$

$$u_1^3 = q_{31} = \frac{G_1}{P_1} a_{32} a_{33} \quad (1\ 2\ 3). \quad (3.6)$$

Here

$$\begin{aligned} \tilde{y}_i &= \sum_{m=1}^4 y_m(t_i); \quad u_3 = u_1 \times u_2; \quad u_i = (u_i^1, u_i^2, u_i^3)^T; \quad u_i^1 = \frac{1}{2} (y_i(t_1) - y_i(t_2)); \\ u_i^2 &= \frac{1}{2P_i} (y_i(t_1) - y_i(t_3)) \quad (i = 1, 2, 3); \quad P_i = A_2 A_3 + B_2 B_3; \\ G_i &= A_2 B_3 - A_3 B_2 \quad (1\ 2\ 3). \end{aligned}$$

Disregarding terms in (3.6) that contain small factors G_i/P_i ($i = 1, 2, 3$), we determine

$$(a_{31}, a_{32}, a_{33})^T = u_3. \quad (3.7)$$

Compensation of drifts of the vectors of kinetic moments $\Delta \omega_i^0$ is realized by subtracting from the preliminary estimates a_{ij}^0 the corrections Δa_{ij}^0 obtained as a result of integrating the error equations

$$\Delta a_{ij}^0 = \tilde{\omega}_i^0 \Delta a_{32}^0 - \tilde{\omega}_2^0 \Delta a_{33}^0 + \Delta \omega_3^0 a_{32}^0 - \Delta \omega_2^0 a_{33}^0 \quad (1\ 2\ 3). \quad (3.8)$$

The problem of smoothing preliminary estimates of the "true" direction cosines d_{ij} that are found from values of a_{ij}^0 after compensation [Ref. 9], and evaluation of ω_i can be reduced to estimation of the vector of state of the system $x = (d_{11}, \dots, d_{33}, \omega_1, \omega_2, \omega_3)^T$ described by Poisson and Euler equations from directly observed preliminary estimates of the d_{ij} . A simpler smoothing procedure assumes use of an approximate model of behavior of the sought variables

$$\dot{x}_1 = x_2 + \xi_1; \quad \dot{x}_2 = x_3 + \xi_2; \dots; \dot{x}_n = \xi_n, \quad (3.9)$$

where $x_1 = (d_{11}, d_{12}, \dots, d_{33}, \omega_1, \omega_2, \omega_3)^T$, ξ_i ($i = 1, 2, \dots, n$) are random gaussian noises. Preliminary estimates of x_1 enable us to formulate the observations

$$y_i = x_1 + \tilde{\xi}_i, \quad (3.10)$$

where $\tilde{\xi}_1$ is the vector of random errors, $y_1 = (y_1^1, y_1^2, \dots, y_1^{12})^T$.

An estimate of the components of vector x_1 for model (3.9), (3.10) can be obtained by using the algorithm of a steady-state linear filter with given attenuation. For example at $n = 4$ we have

$$\hat{x}_i^n = \hat{x}_i^{n-1} + K_i^n \Delta x_i^1; \quad (n = 1, 2, 3); \quad \hat{x}_i^1 = K_i^1 \Delta x_i^1. \quad (3.11)$$

Here

$$\begin{aligned} \hat{x}_r &= (\hat{x}_r^1, \hat{x}_r^2, \dots, \hat{x}_r^{12})^T \quad (r = 1, 2, 3, 4); \quad \Delta x_i^1 = y_i^1 - \hat{x}_i^1; \\ K_i^1 &= 4\lambda_0^1; \quad K_i^2 = 6(\lambda_0^1)^2; \quad K_i^3 = 4(\lambda_0^1)^3; \quad K_i^4 = (\lambda_0^1)^4 \quad (i = 1, 2, \dots, 12); \end{aligned}$$

FOR OFFICIAL USE ONLY

FOR OFFICIAL USE ONLY

λ_0^{-1} is the index of attenuation, i is the number of component \hat{x}_i .

Still another version of the algorithm of smoothing of vector x_i can be obtained by using the approximation of $x_i^{-1}(t)$ on interval ΔT by some series such as

$$x_i^{-1}(t) = \sum_{n=1}^m c_n^i t^n \quad (i = 1, \dots, 12). \quad (3.12)$$

Then, carrying out measurements of x_i^{-1} at fixed points of the interval

$$t_n = n\Delta t \quad (n = 1, 2, \dots, k); \quad \sum_{n=1}^k t_n = \Delta t,$$

we get

$$\hat{c}_i = T^+ u_i, \quad (3.13)$$

where T^+ is the pseudo-inverse matrix;

$$\hat{c}_i = (\hat{c}_0^i, \hat{c}_1^i, \dots, \hat{c}_m^i)^T; \quad u_i = (x_i^{-1}(t_1), x_i^{-1}(t_2), \dots, x_i^{-1}(t_k))^T;$$

$$T = \begin{bmatrix} 1 & \Delta t & (\Delta t)^2 & \dots & (\Delta t)^m \\ 1 & 2\Delta t & (2\Delta t)^2 & \dots & (2\Delta t)^m \\ \dots & \dots & \dots & \dots & \dots \\ 1 & k\Delta t & (k\Delta t)^2 & \dots & (k\Delta t)^m \end{bmatrix}.$$

With such a structure of algorithm (3.13), matrix T^+ can be calculated beforehand from known ΔT , Δt , k and m . The smoothed estimates, and the estimates of the time derivatives of x_i^{-1} are found from estimates of c_n^i with the use of expressions (3.12). On the other hand, estimates of the components of absolute angular velocity ω_i are found from relations stemming from Poisson equations

$$\hat{\Omega}(t) = \hat{D}^T(t) \cdot \dot{D}(t), \quad (3.14)$$

where $\hat{\Omega}$ is a skew-symmetric matrix comprised of ω_i , $i = 1, 2, 3$; $D = \|d_{ij}\|$, \dot{D} are estimates of the orientational matrix D and its derivative that are found by algorithms (3.11), or (3.12), (3.13).

4. The results of numerical solution of the problem considered in sections 2, 3 for data given in Ref. 2, 5 show that errors of reconstruction of the sought motion parameters of the base from the output signals of two electrostatic gyroscopes depend on the accuracy of calibration of parameters appearing in expressions (2.1) and (2.8). When the scheme outlined above is used for solving this problem in the case of conical oscillations of the base with frequency of 1 Hz and amplitude of 0.1 rad at values of $w_1 \approx 20$ m/s², error compensation step of $h = 0.001$ s and relative errors of calibration of the main parameters of the electrostatic gyroscope of ~1%, the errors of reconstruction of projections of the absolute angular velocity of the base do not exceed $5 \cdot 10^{-4}$ 1/s for the steady-state filter algorithm (3.11) at $\lambda_0^{-1} = 100$ s⁻¹, and 10^{-4} 1/s for the approximation algorithm (3.13) at $k = 10$, $\Delta t = 10^{-3}$ s, $m = 4$, while the errors of estimation of d_{ij} are determined mainly by random errors of measurement of rotor displacements of the electrostatic gyroscope relative to the casings.

FOR OFFICIAL USE ONLY

1. Bard, I., "Nelineynoye otsenivaniye parametrov" [Nonlinear Estimation of Parameters], Moscow, Statistika, 1979, 349 pp.
2. Bryushkov, V. G., Martynenko, Yu. G. "Drifts of unbalanced Gyroscope in Electrostatic Suspension of Unequal Stiffness", IZVESTIYA AKADEMII NAUK SSSR: MEKHANIKA TVERDOGO TELA, No 6, 1976, pp 33-40.
3. Martynenko, Yu. G., "Drifts of Electrostatic Gyroscope Caused by Aspherical Rotor", IZVESTIYA AKADEMII NAUK SSSR: MEKHANIKA TVERDOGO TELA, No 1, 1970, pp 10-18.
4. Merkind, D. R., "Giroskopicheskiye sistemy" [Gyroscopic Systems], Moscow, Nauks, 1974, 344 pp.
5. Osipov, Yu. M., Pevzner, Ye. M., Balyasnikova, Ye. M., "Analysis of Disturbing Moments That Act on a Deformed Rotor in an Electrostatic Suspension", IZVESTIYA VYSSHIKH UCHEBNYKH ZAVEDENIY: PRIBOROSTROYENIYE, Vol 17, No 12, 1974, pp 79-88.
6. Plotnikov, P. K., "Izmeritel'nyye giroskopicheskiye sistemy" [Gyroscopic Measurement Systems], Saratov, Saratov University, 1976, 167 pp.
7. Povtorayko, V. I., "Determining Torque Acting on a Rotating Unbalanced Rotor of an Electrostatic Gyroscopic on the Part of the Electrostatic Suspension", TRUDY MOSKOVSKOGO ENERGETICHESKOGO INSTITUTA, No 361, 1978, pp 42-46.
8. Seydzh, E., Mels, Dzh., "Teoriya otsenivaniya i yeye primeneniye v svyazi i upravlenii" [Estimation Theory and its Application in Communications and Control], Moscow, Svyaz', 1976, 495 pp.
9. Christensen, T. W., "Advanced Development of ESG Strapdown Navigation Systems", ELECTRICAL AND ELECTRONICS ENG. TRANS. AEROSPACE AND ELECTRON. SYST., Vol 2, No 2, 1966, pp 143-147.

COPYRIGHT: Izdatel'stvo "Naukova dumka", "Prikladnaya mekhanika", 1981

6610

CSO: 8144/090

- END -